*J. R. Statist. Soc.* B (1999)
**61**, *Part* 1, *pp.* 3–37

# Fractal analysis of surface roughness by using spatial data

Steve Davies

*Commonwealth Scientific and Industrial Research Organisation, Sydney, Australia*

and Peter Hall

*Australian National University, Canberra, Australia*

[*Read before* The Royal Statistical Society *at a meeting organized by the* Research Section *on Wednesday, May 20th, 1998*, Dr D. Draper *in the Chair*]

**Summary.** We develop fractal methodology for data taking the form of surfaces. An advantage of fractal analysis is that it partitions roughness characteristics of a surface into a scale-free component (fractal dimension) and properties that depend purely on scale. Particular emphasis is given to anisotropy where we show that, for many surfaces, the fractal dimension of line transects across a surface must either be constant in every direction or be constant in each direction except one. This virtual direction invariance of fractal dimension provides another canonical feature of fractal analysis, complementing its scale invariance properties and enhancing its attractiveness as a method for summarizing properties of roughness. The dependence of roughness on direction may be explained in terms of scale rather than dimension and can vary with orientation. Scale may be described by a smooth periodic function and may be estimated nonparametrically. Our results and techniques are applied to analyse data on the surfaces of soil and plastic food wrapping. For the soil data, interest centres on the effect of surface roughness on retention of rain-water, and data are recorded as a series of digital images over time. Our analysis captures the way in which both the fractal dimension and the scale change with rainfall, or equivalently with time. The food wrapping data are on a much finer scale than the soil data and are particularly anisotropic. The analysis allows us to determine the manufacturing process which produces the smoothest wrapping, with least tendency for micro-organisms to adhere.

*Keywords*: Fractal dimension; Hausdorff dimension; Isotropy; Local linear estimator; Scale; Topothesy

## 1. Introduction

### 1.1. Overview of fractal methods for surface analysis

The development of statistical methods for analysing surfaces has typically been driven by the technologies used to record data. A relatively old but still rather common approach to measurement is stylus profilometry, in which a fine stylus is drawn across a surface and the current generated by its oscillations is taken as a measure of height. The total electrical charge resulting from these oscillations is proportional to the mean absolute deviation of surface height, not the mean-squared deviation. Therefore, $L^1$-measures of variation can be more attractive than $L^2$-measures, quite apart from any statistical advantages that either might have. More recent technologies allow extensive and detailed surface height data to be recorded and so permit more sophisticated and flexible approaches to data analysis. The new

*Address for correspondence*: Peter Hall, Centre for Mathematics and Its Applications, Australian National University, Canberra, ACT 0200, Australia.
E-mail: Peter.Hall@anu.edu.au

 1369–7412/99/61003

advances include refinements to the performance of stylus profilometers and optical profilometry based, for example, on scanning with a laser or white light from an optical fibre.

However, all profilometer data are recorded from what are essentially line transects of the surface, albeit with a non-infinitesimal width representing the diameter of the stylus or light beam, and so are still rather restrictive. New technologies, such as scanning electron microscopes, allow genuinely two-dimensional data to be gathered, typically in the form of digital images. Such data offer exciting opportunities for addressing issues of anisotropy and spatial variation in a way that is difficult even for extensive profilometer data. This paper is motivated by these possibilities. We suggest new methods for analysing surface data, taking advantage of the new technologies and allowing questions of spatial variability to be addressed.

Our methods are based on semiparametric models for the variogram of stochastic surfaces and allow us to determine those properties that are of particular interest. Among these is the result, derived in Section 3, that the fractal dimension of line transects of a stationary (but not necessarily isotropic) stochastic surface must be invariant in all except a single direction, where it may take a value which is less than that in all other directions. Surfaces which exhibit this 'special' direction are not unlike the sum of a rough ruled surface and a smoother, possibly isotropic, surface: the direction of corrugations of the ruled surface is the unique direction in which the fractal dimension is lower. We shall briefly mention techniques that are appropriate for this and similar examples. In many practical applications, however, it is common for the fractal dimension to be identical in all directions, but for the scale to vary continuously with orientation.

Leaving the issue of anisotropy aside, there are distinct differences between the one- and two-dimensional cases. In one dimension, when $N$ data values are observed at regularly spaced points, ordinary least squares (OLS) estimators based on the variogram are root $N$ consistent and asymptotically normal if and only if the fractal dimension exceeds 1.25 (Constantine and Hall, 1994). We shall show that in two dimensions such estimators are possible only for processes whose one-dimensional transects have fractal dimension exceeding 1.5. There, the analogue of $N$ is the total number of grid points on which the data are digitized. It is possible to improve the performance below these thresholds either by using parametric models (assuming that they are appropriate) or by employing estimators based on generalized least squares (GLS) and high order increments. Details of the latter approach have been given by Kent and Wood (1997), in the case of one dimension. We shall only consider the parametric approach here. The GLS estimators do not perform consistently better than OLS estimators in a range that is close to where the latter attain root $N$ consistency (which includes the context of all the real data sets that we shall consider); indeed, they can perform more poorly.

The new contributions of this paper include a concise account of the potential variation of fractal properties with orientation (Section 3), the development of methods for both isotropic and anisotropic surfaces (Section 4), a numerical and theoretical account of the performance of those methods (Section 5), an illustration of the performance of the methods for real isotropic data (Section 6) and real anisotropic data (Section 7), and bootstrap methods for estimating distributional properties of estimators (Sections 6 and 7).

### 1.2. Related work

There are many ways of characterizing surface roughness, some of them allowing particularly unified or sophisticated treatments (e.g. Whitehouse and Phillips (1982) and Greenwood (1984)). It may be argued, however, that the very sophistication and complexity of some of

these approaches make them awkward to apply or make the results of analysis difficult to interpret (Thomas and Thomas, 1988). Fractal methods (e.g. Berry and Hannay (1978), Berry (1979), Berry and Lewis (1980), Mandelbrot (1982, 1985), Mandelbrot *et al.* (1982), Underwood and Banjeri (1986), Banjeri (1988), Rigaut (1988), Dauskardt *et al.* (1990) and Wang (1997)) are a conceptually simple alternative. They allow the characteristics of surface roughness to be partitioned into two parts, one of them scale invariant and the other governed by properties of scale.

Sayles and Thomas (1977) and Thomas and Thomas (1988), among others, take up issues of spatial properties of surfaces and the potential for anisotropy. Thomas and Thomas (1988) discussed the possibility that the fractal dimension might vary with orientation. The work in the present paper sheds significant light on their analysis. Thomas and Thomas (1988) also addressed mechanisms that might cause self-similarity or self-affineness of surfaces of man-made materials, noting the differing tendencies of different finishing processes to produce fractal-like features. They and others (e.g. Ling (1987, 1989)) address the manner in which the visibility of fractal properties depends on scale.

The literature on surface analysis is vast, with many journals devoted to the topic and some focusing significantly on fractal approaches. A small portion has already been cited. Other items which deserve mention because of either their statistical content or their relative accessibility to a wider scientific audience include Sayles and Thomas (1978), Gilbertson and Zipp (1981), Thomas (1982), Constantine and Hall (1994), Stoyan and Stoyan (1994) and Kent and Wood (1997). Taylor and Taylor (1991) and Ogata and Katsura (1991) addressed the issue of estimating the fractal dimension of curves in one dimension, the latter in the context of spatial patterns. Methods based on spectral analysis, including those of Passoja and Amborski (1978), Passoja and Psioda (1981) and Chan *et al.* (1995), have a connection with time series analysis. Other approaches to the estimation of fractal dimension are based on level crossings (e.g. Feuerverger *et al.* (1994)) and so have links to the theory of stochastic processes (e.g. Cramér and Leadbetter (1963)). There is an extensive and rapidly growing literature on fractal properties connected with the theory of chaos; see for example the papers in the *Journal of the Royal Statistical Society*, series B, on this subject (volume 54, number 2, 1992), and related work such as that of Cutler (1991) and Serinko (1994).

In addition to its application to problems in engineering and physical science (e.g. Thomas and Thomas (1988) and Dubuc *et al.* (1989a, b), the fractal dimension has a rapidly increasing variety of uses in contexts ranging from urban and landscape planning (e.g. Milne (1991a, b)) to oceanography and meteorology (e.g. Jain (1986) and Morrison and Srokosz (1993)), defence science (e.g. Lo *et al.* (1993)) and the study of musical scores (e.g. Hsü and Hsü (1990) and Lewin (1991)).

## 2. Discussion of fractal properties

### *2.1. Fractal dimension, fractal index and topothesy*

There are various definitions of fractal dimension; examples include box counting (e.g. Hall and Wood (1993)) or the Minkowski–Bouligand dimension (e.g. Barnsley (1988), chapter 5, and Taylor and Taylor (1991)) and the Hausdorff dimension (e.g. Adler (1981), chapter 8). See also Massopust (1994), chapter 3. In general, a suitably defined deterministic curve or surface can admit different fractal dimensions, depending on the definition used, or have well-defined dimension according to one approach but not another. However, for the Gaussian-based models that we have in mind, all the common definitions are applicable, and all produce the same numerical value for the dimension.

Let $X$ denote a stationary stochastic process, or random field, whose realization is a $d$-dimensional geometric structure (a curve if $d = 1$ and a surface if $d = 2$), and write

$$\gamma(t) = \text{cov}\{X(t),\, X(0)\}$$

for the covariance at displacement $t$ (a $d$-vector). The Euclidean norm of $t$, $\|t\|$, will be called the lag. The *fractal index* of the process may be defined as the common value $\alpha$ of the real numbers

$$a = \sup\{\xi > 0\colon \gamma(0) - \gamma(t) = O(\|t\|^{\xi}) \text{ as } \|t\| \to 0\}\,,$$
$$b = \inf\{\xi > 0\colon \|t\|^{\xi} = O\{\gamma(0) - \gamma(t)\} \text{ as } \|t\| \to 0\}\,,$$

provided that they do have a common value. In practice it is usual to assume a relatively simple model for the covariance, which ensures equality of $a$ and $b$. For example, in the case of isotropy it may be supposed that

$$\gamma(t) = \gamma(0) - c\|t\|^{\alpha} + o(\|t\|^{\alpha}) \tag{2.1}$$

as $t \to 0$. The value of $\alpha$ always lies between 0 and 2, and (for a Gaussian process or field) equals 2 if $X$ is differentiable.

If the fractal index $\alpha$ is well defined then we put

$$D = d + 1 - \tfrac{1}{2}\alpha\,. \tag{2.2}$$

If the process $X$ is sufficiently closely related to a Gaussian field (see Hall and Roy (1994) for discussion and regularity conditions) then with probability 1 the realizations of $X$ have fractal dimension $D$, using any of the definitions noted earlier. See for example Adler (1981), chapter 8, Sayles and Thomas (1978) and Thomas and Thomas (1988).

Following common terminology for measures of scale, the quantity $c$ at equation (2.1) will be referred to as *topothesy*, from the Greek for 'region'. This terminology does not have a standard meaning, however; note the definitions in Sayles and Thomas (1978), Berry (1979) and Thomas and Thomas (1988). In particular, there are non-equivalent definitions in frequency and spatial domains. In anisotropic cases $c$ may be a function, as we shall show in the next section.

To simplify our theoretical discussion we shall generally suppose that the random curves and surfaces under consideration are stationary, but in many instances this condition is not required, at least for consistency of the estimators of fractal dimension.

### 2.2. Scaling laws and self-similarity

Although often not explicitly stated in work on applications of fractal analysis, formula (2.2) (in the case $d = 1$) is the basis for so-called *scaling laws* that give rise to most of the popular methods for estimating $D$. As the name implies, scaling laws are relationships among properties on different scales — usually an observable macroscopic scale involving an estimable quantity, such as a moment, and a microscopic scale at which sample path fluctuations are difficult to observe directly. Examples of the use of scaling laws for estimation include the log–log-relationships employed to construct estimators via the variogram (as in this paper) or box counting methods.

A random curve, represented as a stochastic function $X(t)$ of position on the line, is *self-similar* if the effect, on all finite dimensional distributions, of a change to the scale of its argument can be undone by an appropriate change of scale of the curve itself, i.e. for each $c > 0$ there is a constant $C = C(c)$ such that all the finite dimensional distributions of $X(ct)$

are identical with those of $C\,X(t)$, modulo a translation. In principle, this definition can be applied to a random surface as well as to a random curve, although, if the notion of a change in scale of the argument is taken to mean identical changes along each axis, the definition is particularly restrictive, requiring the surface to be essentially the projection of a self-similar curve (and so be a ruled surface). The literature is ambiguous about whether self-similarity of a surface should require invariance of finite dimensional distributions under rotations as well as the equivariance of scaling, but this extra degree of symmetry seems to be generally assumed.

It is sometimes argued that the assumption of self-similarity is necessary for developing fractal properties. We disagree, maintaining that it is required only of a hypothetical limiting process that might exist if the scale of measurement were to become infinitely fine. Indeed, the fact that a fractal index is well defined implies that in the limit, as the scale becomes finer, the process $X$ becomes asymptotically self-similar. This, rather than the full force of the self-similarity assumption, is adequate to ensure that the scales in a scaling law do not require explicit specification.

## 3. Variation in fractal properties with direction

### 3.1. Main result

The extent to which the fractal index of line transects of a random field can vary with orientation is particularly limited, as theorem 1 below makes clear. That result asserts that, for any three orientations, the two lowest fractal indices must be identical. Hence, if the fractal dimension can be expressed in terms of the fractal index by the canonical formula (2.2), in the case $d = 1$, then the two highest values of the fractal dimension must be equal. Since equation (2.2) is a prerequisite for scaling laws, we may say that

> 'if the stationary stochastic surface $X$ satisfies the usual one-dimensional scaling laws then the fractal dimensions of its line transect processes are the same in all directions except possibly one, whose dimension may be less than in all others'.

See also Hall and Davies (1995).

*Theorem 1.* Let $\gamma$ denote a covariance function in the plane with the property that, for any three different orientations $\theta_1$, $\theta_2$ and $\theta_3$ (denoting unit vectors such that $\theta_i \neq \pm\theta_j$ for $i \neq j$), the quantities

$$a_i = \sup\{\alpha > 0 : \gamma(0) - \gamma(u\theta_i) = O(|u|^\alpha) \text{ as } u \to 0\}\,,$$
$$b_i = \inf\{\alpha > 0 : |u|^\alpha = O\{\gamma(0) - \gamma(u\theta_i)\} \text{ as } u \to 0\}$$

satisfy $a_i = b_i$ $(= \alpha_i$, say). Order the $\theta_i$ so that $\alpha_1 \leqslant \alpha_2 \leqslant \alpha_3$. Then $\alpha_1 = \alpha_2$.

*Proof.* Let $c_1$, $c_2$ and $c_3$ denote real numbers such that $\Sigma\, c_i = 0$ and $c_1 c_2 > 0$. Let $u_1$, $u_2$ and $u_3$ be non-zero real numbers such that, with $\omega_i = u_i\,\theta_i$, we have $\Sigma\,\omega_i = 0$. Given $u > 0$, put $t_1 = 0$, $t_2 = u\omega_1$ and $t_3 = u(\omega_1 + \omega_2)$. Define $\delta(t) = \gamma(0) - \gamma(t)$. Let $X$ denote a stationary process with covariance $\gamma$. Now,

$$0 \leqslant \operatorname{var}\{\textstyle\sum c_i\, X(t_i)\} = \sum\sum c_i c_j\,\gamma(t_i - t_j) = -\sum\sum c_i c_j\,\delta(t_i - t_j)$$
$$= -2\{c_1 c_2\,\delta(t_1 - t_2) + c_2 c_3\,\delta(t_2 - t_3) + c_3 c_1\,\delta(t_3 - t_1)\}\,.$$

Suppose that, contrary to the claim of theorem 1, $\alpha_1 < \alpha_2 \leqslant \alpha_3$. Divide both sides of the inequality above by $\delta(t_1 - t_2)$, and let $u \to 0$, obtaining $0 \leqslant -2c_1 c_2$, which contradicts the assumption that $c_1 c_2 > 0$.

### 3.2. Discussion

A result related to theorem 1, that the fractal dimension is the same in 'almost all' directions with respect to Lebesgue measure, is given in the non-stationary case by Marstrand (1954), Falconer (1985), chapter 6, and Mattila (1985). The more specific result in theorem 1, that the fractal dimension is the same in all directions except possibly one, is of significantly greater physical interest because most man-made surfaces are produced in a manner that ascribes special importance to a particular 'manufacturing axis'. Thus, it is feasible that an orientation of special fractal character might exist. Materials that have been milled, ground, face tuned or bored often have surfaces that closely resemble the mathematical ideal of a ruled surface. After processing, they are not unlike the superposition of a ruled surface and a stationary, stochastic, isotropic surface. See example 3.

These direction invariance properties may be regarded as the basis for a physical measurement of surface roughness based on stylus or optical profiling. If one's goal is the estimation of the fractal dimension, as distinct from scale, then it is often not essential to be meticulous about the orientation of a profile. Nevertheless, even if the dimension of line transects is the same in all directions, it can be statistically beneficial to take measurements in the direction in which the scale of fluctuations is greatest.

We stress that, even in cases where the fractal dimension of line transect samples can assume different values in different directions, the fractal dimension of the surface $\{X(t), t \in \mathbb{R}^2\}$ 'as a whole' is usually well defined and equals 1 plus the higher of the two fractal dimensions of line transect sections: see for example Fedderer (1969), section 3.10.

The dependence of scale on orientation is more complex but may be appreciated from a version of equation (2.1) without assuming isotropy. If $d = 2$ then equation (2.1) should generally be replaced by

$$\gamma(t) = \gamma(0) - c\{\arg(t)\}\|t\|^{\alpha} + o(\|t\|^{\alpha}), \tag{3.1}$$

where $\arg(t)$ denotes the angle made by the 2-vector $t$ to a fixed direction in the plane; $c\{\arg(t)\}$ is a continuous, periodic and non-negative function, non-degenerate in the case of anisotropy, and $0 < \alpha \leqslant 2$ is a constant. The function $c\{\cdot\}$ is strictly positive except possibly for a single special value, say $\omega_0$, of $\arg(t)$, where $c\{\arg(t)\}$ vanishes. The fractal index and fractal dimension for line transect samples in this direction are determined by the form of the remainder term $o(\|t\|^{\alpha})$ when $\arg(t) = \omega_0$. In all other directions they equal $\alpha$ and $2 - \frac{1}{2}\alpha$ respectively. Note particularly that in the case of equation (3.1) $c$ is a function — the topothesy function. Compare the discussion of topothesy in Section 2.2.

### 3.3. Examples

In the first example, based on the sum (or convolution) of a finite number of stochastic ruled surfaces, the fractal index can be different in one direction; in the second, $\{\gamma(0) - \gamma(t)\} \sim \frac{1}{2}\, c\{\arg(t)\}\, \|t\|^{\alpha_0}$, where $c$ is a positive non-degenerate function and $0 < \alpha_0 \leqslant 2$. The third example addresses fractal properties of the sorts of highly directional surfaces that arise in practice.

Let $\Theta$ denote the set of all unit vectors in $\mathbb{R}^2$. For an arbitrary distribution function $F$ on the interval $(0, 1)$ and arbitrary functions $a$: $(0, 1) \to [0, \infty)$, $\alpha$: $(0, 1) \to (0, 2]$ and $\theta$: $(0, 1) \to \Theta$, the quantity

$$\gamma(t) = \int_0^1 \exp\{-a(s)\, |\theta(s)^{\mathrm{T}}\, t|^{\alpha(s)}\}\, \mathrm{d}F(s) \tag{3.2}$$

is a covariance function, since it is a convex combination of covariance functions.

If $\gamma$ is given by equation (3.2) and if $\int a^2 \, \mathrm{d}F < \infty$ then the variogram,

$$v(t) = E\{X(t) - X(0)\}^2 = 2\{\gamma(0) - \gamma(t)\},$$

satisfies

$$v(t) = 2 \int_0^1 a(s) \, |\theta(s)^{\mathrm{T}} \, t|^{\alpha(s)} \, \mathrm{d}F(s) + O\left\{ \int_0^1 a(s)^2 \, |\theta(s)^{\mathrm{T}} \, t|^{2\alpha(s)} \, \mathrm{d}F(s) \right\}$$

as $\|t\| \to 0$.

*3.3.1. Example 1*

Consider a sequence $X_1, \ldots, X_m$ of independent stationary stochastic processes on the line, with respective covariance functions $\gamma_i(u) = \exp(-a_i|u|^{\alpha_i})$, where $0 < \alpha_1 \leqslant \ldots \leqslant \alpha_m \leqslant 2$. Then the process

$$X(t) = m^{-1/2} \sum_{i=1}^{m} X_i(\theta_i^{\mathrm{T}} t) \tag{3.3}$$

is a sum of independent ruled surfaces and has covariance function of the form at equation (3.2), with a discrete $F$. If $m = 1$, or if $m \geqslant 2$ but $\theta_i = \pm\theta_1$ for each $2 \leqslant i \leqslant m$, then the process $X$ is a ruled surface and all its stochastic behaviour is in the direction of $\theta_1$. To avoid this uninteresting case we assume that $m \geqslant 2$ and, for some $i \geqslant 2$, $\theta_i \neq \pm\theta_1$.

Suppose that there are just $k$ $\alpha_i$ equal to $\alpha_1$, i.e. $\alpha_1 = \ldots = \alpha_k < \alpha_{k+1}$.

(a) When $k \geqslant 2$ and $\theta_i \neq \pm\theta_1$ for some $2 \leqslant i \leqslant k$,

$$v(t) \sim 2 \, c\{\arg(t)\} \, \|t\|^{\alpha_1}$$

as $\|t\| \to 0$, where, if $\omega$ is a unit vector in the direction of $t$,

$$c\{\arg(t)\} = m^{-1} \sum_{i=1}^{k} a_i \left|\theta_i^{\mathrm{T}} \, \omega\right|^{\alpha_1},$$

and $\inf_t[c\{\arg(t)\}] > 0$. It follows that the fractal index of line transect processes derived from $X$ equals $\alpha_1$ in all directions.

(b) When $k = 1$, or $k \geqslant 2$ and $\theta_i = \pm\theta_1$ for $2 \leqslant i \leqslant k$, put

$$l_1 = \inf\{i \geqslant k+1\text{: for all } 1 \leqslant j \leqslant k, \, \theta_i \neq \pm\theta_j\},$$
$$l_2 = \sup\{i \geqslant k+1\text{: } \alpha_i = \alpha_{l_1}\}.$$

If $\omega \in \Theta$ is not perpendicular to $\theta_1$ then

$$v(u\omega) \sim 2\left(m^{-1} \sum_{i=1}^{k} a_i\right) \left|\theta_1^{\mathrm{T}} \, \omega\right|^{\alpha_1} |u|^{\alpha_1}$$

as $u \to 0$, and, if $\omega \perp \theta_1$,

$$v(u\omega) \sim 2\left(m^{-1} \sum_{i=l_1}^{l_2} a_i \left|\theta_i^{\mathrm{T}} \, \omega\right|^{\alpha_{l_1}}\right) |u|^{\alpha_{l_1}}$$

as $u \to 0$. It follows that the fractal index of line transect processes equals $\alpha_1$ in all directions except those orthogonal to $\theta_1$, in which case it equals $\alpha_{l_1}$.

In practice it would seldom be possible to confirm the existence of a high order model such as process (3.3), unless the amount of data was considerable. In particular, an estimation of the $\alpha_i$ is virtually equivalent to an estimation of high order terms in an expansion of the covariance function of $X$ in the neighbourhood of the origin, and it is seldom practicable to go beyond the first one or two terms. Certainly, fractal methods address only these components of the series at equation (3.3).

### 3.3.2. *Example 2*

Consider the general mixture model (3.2), in which $\alpha \equiv \alpha_0$ is fixed, $F$ is supported on $[0, 1]$ and $\theta(\cdot)$ is non-degenerate. Given $t \in \mathbb{R}^2$ let $\omega$ denote a unit vector in the direction of $t$, and define

$$c\{\arg(t)\} \equiv \int_0^1 a(s)\,|\theta(s)^{\mathrm{T}}\,\omega|^{\alpha_0}\;\mathrm{d}F(s)\,.$$

Then

$$v(t) = 2\,c\{\arg(t)\}\,\|t\|^{\alpha_0} + O(\|t\|^{2\alpha_0})$$

as $t \to 0$. Therefore, as in case (a) of example 1, the fractal indices of line transect processes are identical in all directions, and the topothesy function $c$ can be non-degenerate.

### 3.3.3. *Example 3*

Approximations to perfect ruled surfaces (of the type in example 1 with $m = 1$) are sometimes encountered in real life. See for example Stout *et al.* (1993). However, they always have a little off-axis variability, which is captured by the artificially shaded image of a simulated bored or ground engineering surface in Fig. 1. Fig. 1 was obtained by adding isotropic and ruled surfaces, both generated on a $256 \times 256$ grid covering the unit square. The isotropic surface was a realization of a Gaussian random field with covariance function $\gamma(t) = \exp(-8\|t\|^{3/2})$.

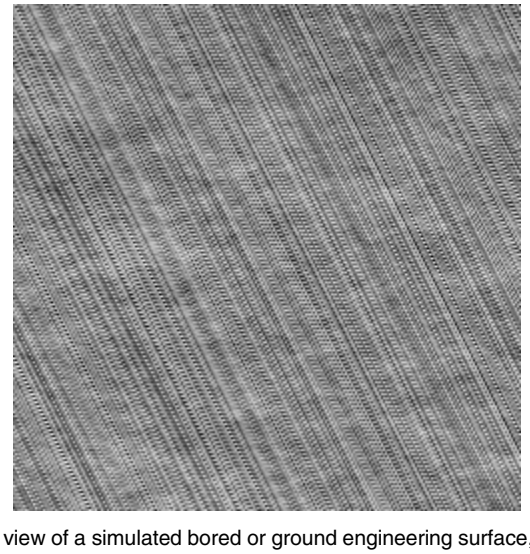

**Fig. 1.** Artificially shaded view of a simulated bored or ground engineering surface, exhibiting two distinct fractal dimensions

The ruled surface was constructed by simulating a one-dimensional Gaussian process with covariance function $\gamma(t) = \exp(-\frac{1}{2}\|t\|^{1/2})$ along the line $\mathcal{L}$ defined by the equation $y = x/2$, and then projecting this process perpendicularly to $\mathcal{L}$. Transects of the resulting surface have fractal dimension $1\frac{3}{4}$ in all directions except that orthogonal to $\mathcal{L}$, where the dimension is $1\frac{1}{4}$. Fig. 2 shows that the variation in fractal dimension is evident empirically. Larger lags are represented by the dotted lines in Fig. 2.

## 4. Models and methods

### 4.1. Isotropic case

For the most part our approach to estimating fractal dimension and topothesy of a random surface $X$ is based on the variogram, although methods such as box counting perform similarly. See Davies (1998), chapter 5. When $X$ is isotropic, $v(t)$ is a function of $\|t\|$, and we shall write $v(\|t\|)$ for $v(t)$ (with a slight abuse of notation).

Assume that the covariance of $X$ satisfies equation (2.1), or equivalently

$$\log\{v(t)\} = \log(2c) + \alpha \log(\|t\|) + o(1) \tag{4.1}$$

as $t \to 0$. Then estimates $\hat{\alpha}$ of fractal index and $\hat{c}$ of topothesy are based on the slope and intercept respectively of the linear regression $\log\{v(t)\} \approx \log(2c) + \alpha \log(\|t\|)$ at small lags.

In view of equation (2.2), an estimator $\hat{\alpha}$ of fractal index may be converted into an estimator $\hat{D}$ of fractal dimension by substituting into the formula

$$\hat{D} = d + 1 - \tfrac{1}{2}\hat{\alpha}\,. \tag{4.2}$$

We construct two unbiased estimators of the variogram: $\hat{v}_{\mathrm{I}}$ under the assumption of

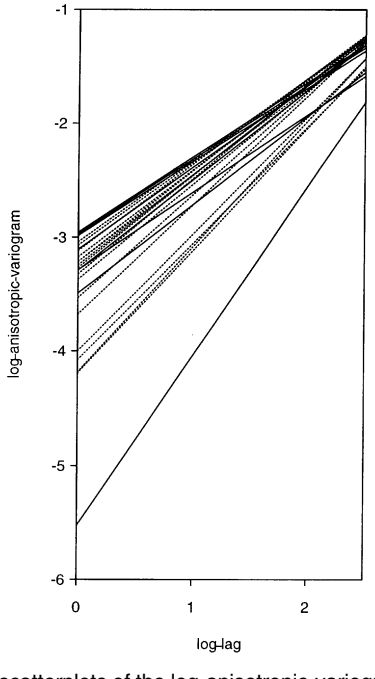


**Fig. 2.** Least squares fits to scatterplots of the log-anisotropic-variogram $\hat{v}_{\mathrm{A}}$ against the log-lag for line transects in different directions for the data depicted in Fig. 1: ·····, fits based on larger lags

isotropy and $\hat{v}_A$ more generally. Assume that $X$ is observed on an $m \times n$ regular lattice, at points $t_{ij}$, $1 \leqslant i \leqslant m$, $1 \leqslant j \leqslant n$. (In practice these values of $X$ are usually averages, although not strict pixel averages; the area over which the average is taken can be much smaller than that of a pixel.) Given $u > 0$ and $t \in \mathbb{R}^2$, define $\mathcal{S}_I(u) = \{(i, j, k, l)\colon \|t_{ij} - t_{kl}\| = u\}$, $\mathcal{S}_A(t) = \{(i, j, k, l)\colon t_{ij} - t_{kl} = t\}$, $N_I(u) = \#\mathcal{S}_I(u)$ and $N_A(t) = \#\mathcal{S}_A(t)$; and if $N_I(u)$, $N_A(t) \geqslant 1$, put

$$\hat{v}_I(u) = N_I(u)^{-1} \sum_{(i,j,k,l)\in\mathcal{S}_I(u)} \{X(t_{ij}) - X(t_{kl})\}^2,$$

$$\hat{v}_A(t) = N_A(t)^{-1} \sum_{(i,j,k,l)\in\mathcal{S}_A(t)} \{X(t_{ij}) - X(t_{kl})\}^2.$$

The performances of $\hat{v}_I(u)$ and $\hat{v}_A(t)$ depend, among other things, on the sizes of $N_I(u)$ and $N_A(t)$, which can range from 1 to $O(mn)$.

Variogram estimators of this form are of course standard in other spatial applications of statistics; see for example Cressie (1991), p. 40 and following feature, who surveys some applications of the variogram and discusses related methods (including the robust variogram). Cressie (1991), p. 40, also draws connections to intrinsic stationarity, and (on p. 58 and the following feature and chapter 3) to kriging methods. Intrinsic stationarity — i.e. the assumption that the variogram depends only on the vector value of the lag — is all that is required to define the fractal index.

Let $u_1, \ldots, u_k$ denote $k$ positive numbers such that each $N_I(u_i)$ is greater than or equal to 1. We estimate $\alpha$ as the slope, and $\log(2c)$ as the intercept, in OLS linear regression of $\log\{\hat{v}_I(u_i)\}$ on $\log(u_i)$:

$$\hat{\alpha} = \sum_{i=1}^{k} \log\{\hat{v}_I(u_i)\}\{\log(u_i) - \overline{\log(u)}\} \Big/ \sum_{i=1}^{k} \{\log(u_i) - \overline{\log(u)}\}^2, \tag{4.3}$$

$$\hat{c} = \tfrac{1}{2} \exp\Big[k^{-1} \sum_{i=1}^{k} \log\{\hat{v}_I(u_i)\} - \hat{\alpha}\,\overline{\log(u)}\Big], \tag{4.4}$$

where $\overline{\log(u)} = k^{-1} \Sigma \log(u_i)$.

### 4.2. Anisotropic case

We suggest two methods of analysis, the first an analogue of the nonparametric approach suggested in Section 4.1 but tailored to the estimation of topothesy, and the second based on fitting a semiparametric model to the variogram. In the nonparametric context we use the estimator $\hat{\alpha}$ defined at equation (4.3), which is appropriate in the anisotropic case provided that the function $c(\cdot)$ in equation (3.1) is bounded away from 0 (or equivalently that the fractal dimension is constant in all directions). Then, we estimate $c(\theta)$ for a discrete sequence of orientations, and we use a standard smoothing method to approximate the function $c(\cdot)$.

Let $\theta_1, \ldots, \theta_\nu$ denote $\nu$ distinct orientations that represent lines through points on the square lattice; let $u_{ij}$, for $1 \leqslant j \leqslant k_i$, be positive scalar values such that each $N_A(u_{ij}\,\theta_i) \geqslant 1$; put $c_i = c\{\arg(\theta_i)\}$. Let $\hat{\alpha}$ be as defined at equation (4.3) (we are continuing to define $\hat{\alpha}$ as in the isotropic case), and analogously to the definition at equation (4.4) put

$$\hat{c}_i = \tfrac{1}{2} \exp\Big[k_i^{-1} \sum_{j=1}^{k_i} \log\{\hat{v}_A(u_{ij}\,\theta_i)\} - \hat{\alpha}\,\overline{\log(u_i)}\Big], \tag{4.5}$$

where $\overline{\log(u_i)} = k_i^{-1} \Sigma_j \log(u_{ij})$. For general $\phi \in (-\pi/2, \pi/2)$, define $\hat{c}(\phi)$ by passing a local linear smoother (Fan, 1993; Hastie and Loader, 1993) through the pairs of points $(\theta_i, \hat{c}_i)$,

using a compactly supported kernel $K$ and interpreting both $\phi$ and $\arg(\theta_i)$ as though they took values on the interval $(-\pi/2, \pi/2)$ wrapped around a circle.

A semiparametric model may be based on the assumption of an elliptically contoured variogram, sometimes termed 'weak anisotropy'. We formulate this mathematically in terms of the following approximation to the variogram near the origin:

$$\log\{v(t)\} = \log(c_0) + \frac{\alpha}{2}\log(1 + s\cos[2\{\arg(t) - \psi\}]) + \alpha\log(\|t\|). \tag{4.6}$$

(Having computed an estimator $\hat{\alpha}$ of $\alpha$ via the model at equation (4.6), we define $D$ as suggested at equation (4.2).) The parameter $s$ lies between 0 and 1 and provides a measure of the strength of anisotropy of a surface. A value of 0 for $s$ would result in the topothesy function degenerating to a constant and hence would imply the expansion (4.1) of the variogram of an isotropic process, i.e. no anisotropy in a local sense. A value of 1 for $s$ would be appropriate for the variogram of a ruled surface, i.e. complete anisotropy. If $s$ were non-zero then $\psi$, which we might call the 'lay', would be the orientation at which the topothesy function attained its maximum value. If there existed a direction in which the fractal dimension took a unique value, different from that in all other directions, then it would be orthogonal to that defined by $\psi$. We may consider $c_0$ to be the 'average topothesy'.

## 5. Performance of estimators

### 5.1. Discussion of convergence rates

Consider a two-dimensional Gaussian random field $X$ observed at points $t_{ij}$ on an $n \times n$ square grid with edge width $n^{-1}$. We shall show that, under mild assumptions which include that

$$\gamma(t) = \gamma(0) - c\|t\|^{\alpha}\{1 + r\|t\|^{\beta} + o(\|t\|^{\beta})\} \tag{5.1}$$

as $t \to 0$ (where $c > 0$, $r$ is real, $0 < \alpha \leqslant 2$ and $\beta > 0$), the OLS estimators $\hat{\alpha}$ and $\hat{c}$, defined at equations (4.3) and (4.4), satisfy

$$\hat{\alpha} - \alpha = O_p(n^{\alpha-2}\lambda_n + n^{-\beta}), \tag{5.2}$$

$$\hat{c} - c = O_p\{(n^{\alpha-2}\lambda_n + n^{-\beta})\log(n)\} \tag{5.3}$$

as $n \to \infty$, where

$$\lambda_n = \begin{cases} 1 & \text{if } 1 < \alpha < 2, \\ \log(n)^{1/2} & \text{if } \alpha = 1, \\ n^{1-\alpha} & \text{if } 0 < \alpha < 1. \end{cases} \tag{5.4}$$

These results make explicit the way in which the convergence rates of $\hat{\alpha}$ to $\alpha$ and $\hat{c}$ to $c$ are determined by both $\alpha$ and $\beta$.

The first term in equation (5.2) represents the contribution from error about the mean, whereas the second term describes the contribution from bias. If $\alpha > 1$, the term involving the error about the mean dominates the bias term if and only if $\alpha + \beta > 2$, whereas for $\alpha < 1$ the relevant condition is $\beta > 1$. In the important special case where $\gamma(t) = \exp(-c\|t\|^{\alpha})$ we have $\alpha = \beta$, and so the term involving the error about the mean of $\hat{\alpha}$ dominates its bias if and only if $\alpha \geqslant 1$.

The rates of convergence of estimators of $\alpha$ and $c$ deteriorate as $\alpha$ becomes close to 2, because the amount of information contained in oscillations of $X$ decreases as the process

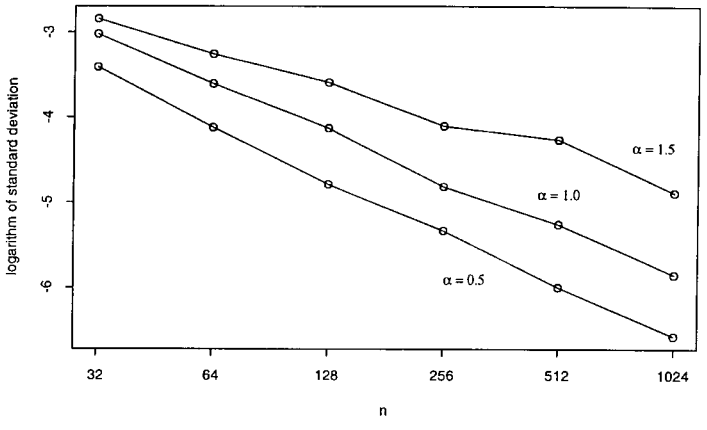


(a)

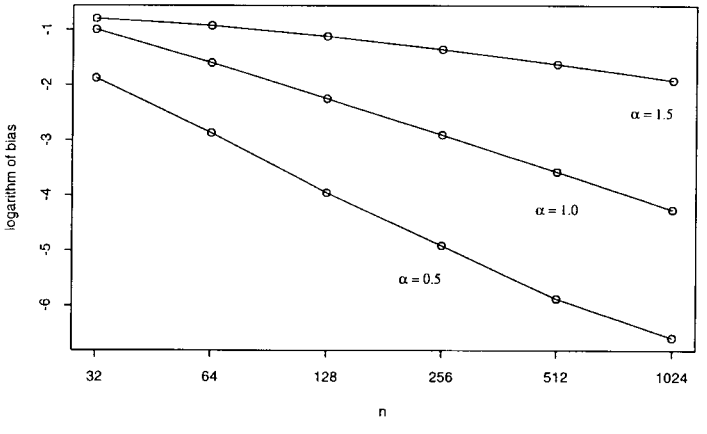


(b)

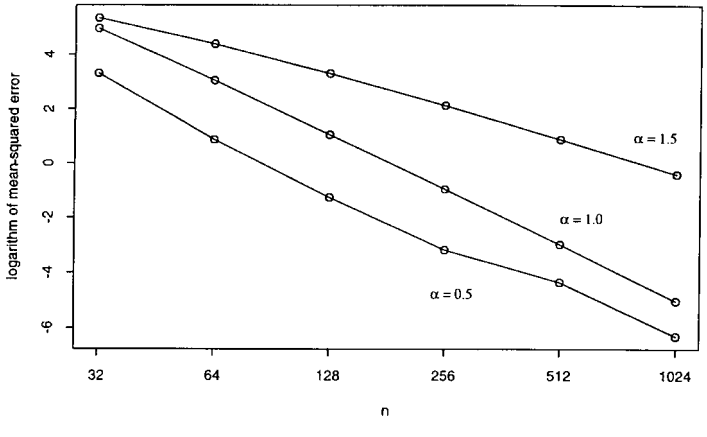


(c)

**Fig. 3.** Plots of logged standard error, bias and mean-squared error as a function of the logarithm of the sample size, for a two-dimensional Gaussian random field with covariance $\gamma(t) = \exp(-16\|t\|^{\alpha})$ and for various values of $\alpha$

becomes smoother. In an extreme case, if $\alpha = 2$ then there is insufficient information in a record of $X$ on a finite interval to estimate $c$ consistently. As $\alpha$ increases to 2, we need to examine successively higher order properties to obtain a similar performance; see Kent and Wood (1997). The problems as $\alpha$ approaches 2 are observable in a simulation study, such as that summarized in Fig. 3. Fig. 3(a) depicts the logarithm of the standard error of $\hat{\alpha}$, Fig. 3(b) the logarithm of the bias in $\hat{\alpha}$ and Fig. 3(c) the logarithm of the mean-squared error of $\hat{\alpha}$, plotted against $\log(n)$ for $\alpha = 0.5$, 1.0, 1.5. Data were generated from a two-dimensional Gaussian random field with covariance $\gamma(t) = \exp(-16\|t\|^{\alpha})$, in the range $t \in [0, 1]^2$. We took $k = 4$ and $u$ to equal $n^{-1}$ multiplied by one of 1, $2^{1/2}$, 2 and $2^{3/2}$. For respective values of $n$ the curves were based on $4(1024/n)^2$ simulations. For $\alpha > 1$, the performance deteriorates as $\alpha$ increases, owing to an increase in variance, whereas, for $\alpha < 1$, the performance improves with increasing $\alpha$, owing to a decrease in bias.

In addition to saving computational labour, there are two reasons for choosing $k$ relatively small. First, it minimizes bias from the $o(1)$ term in equation (4.1). Secondly, estimates of the variogram exhibit high correlation between values at neighbouring lags, and using more lags in the regression does not improve the accuracy of estimates as much as in the case of data with lower correlation. Indeed, taking the number of points in the regression to diverge with increasing sample size will inflate both the bias and the variance, and so even in an asymptotic sense, as $n \to \infty$, the optimal $k$ is bounded. This has been shown theoretically by Constantine and Hall (1994). To provide a numerical illustration, Fig. 4 depicts a plot of mean-squared error of $\hat{\alpha}$ against $k$, in the case of a Gaussian process on the interval [0, 1] with covariance $\gamma(t) = \exp(-16|t|^{\alpha})$ and $\alpha = 1.25$. Clearly, the mean-squared error performance is optimized at a relatively small value, $k = 2$. Similar results are obtained in the bivariate case.

The amount of data on the $n \times n$ grid is of the order $n^2$, and so a convergence rate of $\hat{\alpha} - \alpha = O_p(n^{-1})$ corresponds to root $N$ consistency in more classical problems. If $\beta \geqslant 1$, this rate is attained in equation (5.2) if and only if $0 < \alpha < 1$. Broadly similar behaviour may be observed in the case of inference about fractal dimension in one-dimensional processes (Constantine and Hall, 1994), except that the dividing line between root $N$ consistency and a slower convergence rate occurs at $\alpha = \frac{3}{2}$, not $\alpha = 1$.

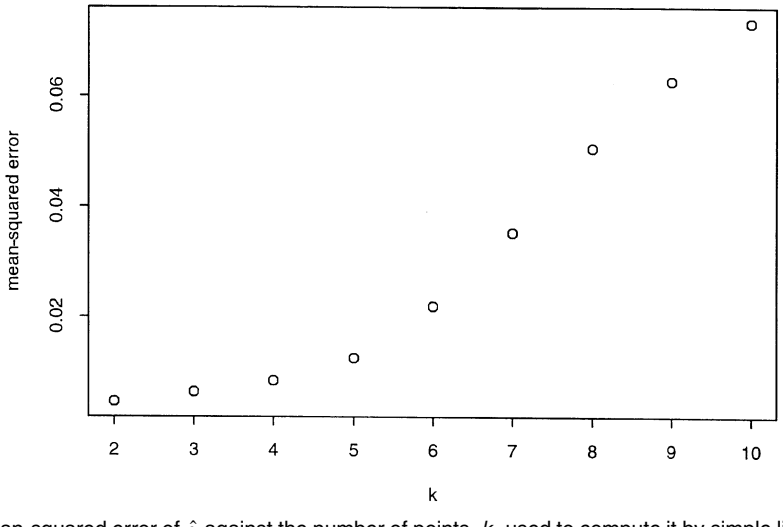


**Fig. 4.** Mean-squared error of $\hat{\alpha}$ against the number of points, $k$, used to compute it by simple linear regression: the data were from a Gaussian process with covariance $\gamma(t) = \exp(-16|t|^{1.25})$

The estimators $\hat{\alpha}$ and $\hat{c}$ are not consistent when $\alpha = 2$, and the Gaussian model is not well defined when $\alpha = 0$.

In both contexts these respective values of $\alpha$ also represent the dividing line between circumstances where $\hat{\alpha}$ is asymptotically normally distributed and those where it is not, with normality occurring for values of $\alpha$ less than the critical value. This is of some practical significance, since many of the real bivariate data sets that we have encountered are well approximated by processes having $\alpha$ between 1 and $\frac{3}{2}$.

### 5.2. Technical results about convergence rates

The assumptions used to guarantee the convergence rates at equations (5.2) and (5.3) are that equation (5.1) holds, that

$$\max_{(i,j)=(1,1),(2,2),(1,2)} |(\partial^2/\partial t^{(i)}\,\partial t^{(j)})\,\gamma(t)| = O(\|t\|^{\alpha-2}) \tag{5.5}$$

and that there are constants $0 < a_1 < \ldots < a_k$ and $b_1, \ldots, b_k > 0$ such that, for $1 \leqslant i \leqslant k$, $a_i$ and $b_i$ satisfy

$$u_i \sim a_i n^{-1} \quad \text{and} \quad N_{\mathrm{I}}(u_i) \sim b_i n^2. \tag{5.6}$$

Condition (5.6) is typically satisfied in practice. For example, if $a_1, \ldots, a_k$ are taken to be distinct, and are chosen from among the set of all lengths of diagonals of a square grid with unit side width, e.g. $2^{1/2}$, $5^{1/2}$, $8^{1/2}$, . . ., or from the set of all positive integers, and if $u_i = a_i n^{-1}$ for $1 \leqslant i \leqslant k$, then condition (5.6) holds. Condition (5.5) is no more than a second-derivative version of the elementary assumption that $\gamma(t) = \gamma(0) + O(\|t\|^{\alpha})$, implied by equation (5.1), and is likewise a mild assertion. In particular, it follows if $\gamma(t) = \exp(-c\|t\|^{\alpha})$ for some $c > 0$ and $0 < \alpha \leqslant 2$.

To establish the convergence rates in equations (5.2) and (5.3), observe that we may write

$$\log\{\hat{v}_{\mathrm{I}}(u)\} = \log(2c) + \alpha\,\log(u) + \delta(u) + \epsilon(u),$$

where $\epsilon(u) = \log\{\hat{v}_{\mathrm{I}}(u)/v(u)\}$ represents stochastic error and has virtually zero mean, and $\delta(u) = \log\{v(u)/2cu^{\alpha}\}$ represents the majority of the bias. Under condition (5.1), $\delta(u) \sim \mathrm{d}u^{\beta}$ as $u \to 0$, and the following theorem describes the size of $\epsilon(u)$.

*Theorem 2.* Under conditions (5.1)–(5.6), and assuming that $0 < \alpha < 2$ and $X$ is Gaussian, $\epsilon(u) = O_p(n^{\alpha-2}\,\lambda_n) = o_p(1)$ as $n \to \infty$.

Collating the sizes of stochastic error and bias yields

$$\log\{\hat{v}_{\mathrm{I}}(u)\} = \log(2c) + \alpha\,\log(u) + O_p(n^{\alpha-2}\,\lambda_n + n^{-\beta}),$$

from which follow conditions (5.2) and (5.3).

### 5.3. Asymptotic distributions

Longer technical arguments may be used to show that, if $r$ in equation (5.1) is non-zero, the convergence rates described by equations (5.2) and (5.3) are exact, in the sense that there exist non-zero constants $C_1$ and $C_2$, and random variables $Y_{n1}$ and $Y_{n2}$ with non-degenerate limiting distributions, such that

$$\hat{\alpha} - \alpha = n^{\alpha-2}\lambda_n Y_{n1} + \{1 + o(1)\}\, C_1\, n^{-\beta}, \tag{5.7}$$

$$\hat{c} - c = [n^{\alpha-2}\lambda_n Y_{n2} + \{1 + o(1)\}\, C_2\, n^{-\beta}]\log(n). \tag{5.8}$$

The limiting distributions of $Y_{n1}$ and $Y_{n2}$ are normal only when $\alpha \leqslant 1$; for $\alpha > 1$ they are related to distributions first discussed by Rosenblatt (1961). Similar limit theorems may be derived when $X$ is a function of a Gaussian process, such as a $\chi^2$-process.

Details of asymptotic properties and their derivation will appear in Davies (1998). Here we give an outline of a typical proof in the case $1 < \alpha < 2$, and an indication of the nature of the limiting distribution. First we consider the anisotropic case, since the isotropic case is derived directly from it. Note that for each $r \geqslant 1$ the $r$th cumulant of $n^2\, \hat{v}_A(s_1/n, s_2/n)$, for scalar $s_1$ and $s_2$, converges to a proper limit, $\kappa_r = \kappa_r(s_1, s_2)$ say. We may express $\kappa_r$ as follows. Let $V_{1,pq}$ denote the second derivative of $v$ with respect to the $p$th and then the $q$th component of its argument, let $V_{2,pq} = s_p s_q V_{1,pq}$ and let $V$ equal the sum of $V_{2,pq}$ over all four pairs $(p, q)$. Given 2-vectors $x_1, \ldots, x_r$, let $W(x_1, \ldots, x_r)$ equal the product of $V(x_j - x_{j+1})$ over $1 \leqslant j \leqslant r$, with $x_{r+1}$ interpreted as $x_1$. Then, regarding $W(x_1, \ldots, x_r)$ as a function $U$ of the $2r$ components of the $x_i$, $\kappa_r$ equals $2^{r-1} \times (r-1)!$ multiplied by the integral of $U$ over $[0, 1]^{2r}$. These cumulants are closely related to those derived by Taqqu (1975), who noted the relationship of their parent distribution to finite dimensional distributions of stochastic processes introduced by Rosenblatt (1961).

Continuing this argument, it is conceptually simple but algebraically tedious to derive the $r$th multivariate cumulant of the limiting distribution of $n^2\, \hat{v}_A(s_1/n, s_2/n)$, for all pairs $(s_1, s_2)$ that arise by solving the equations $(s_1^2 + s_2^2)^{1/2} = a_i$ where the $a_i$ are as at condition (5.6). The joint limiting distribution, $F$ say, of these values of $n^2\, \hat{v}_A(s_1/n, s_2/n)$ may be defined in this way. The limiting distributions of $Y_{n1}$ and $Y_{n2}$ may be expressed as a functional of $F$.

Univariate versions of these results, and in particular equations (5.7) and (5.8), are given by Matthews (1998). See also Kent and Wood (1997), who discussed the differences between estimators based on OLS and GLS in the case $d = 1$.

The estimator $\hat{c}_i$, defined in Section 4, has many of the properties of $\hat{c}$, introduced in Section 3. Indeed, assume that as $n$ increases the values of $\theta_i$ and $k_i$ are kept fixed, even though the number $\nu = \nu(n)$ of distinct orientations $\theta_i$ may diverge. Let $u_{i1}, \ldots, u_{ik_i}$ and $\theta_i$ satisfy the directional analogue of condition (5.6):

$$u_{ij} \sim r_{ij}\, n^{-1} \quad \text{and} \quad N_A(u_{ij}\, \theta_i) \sim s_{ij}\, n^2.$$

It is sufficient that the vectors $nu_{ij}\, \theta_i$ represent displacements between vertices on the square lattice with unit side length. For the covariance function $\gamma$, assume conditions (5.5) and, in place of assumption (5.1),

$$\gamma(t) = \gamma(0) - c\{\arg(t)\}\|t\|^{\alpha}\{1 + O(\|t\|^{\beta})\}.$$

Define $\lambda_n$ by equations (5.4). Then it may be shown, much as in the proof of theorem 2, that

$$\hat{c}_i - c_i = O_p\{(n^{\alpha-2}\, \lambda_n + n^{-\beta})\, \log(n)\}.$$

Compare equation (5.3). It may further be proved that, if the function $c$ is non-vanishing and continuous in a periodic sense, if $\nu \to \infty$ sufficiently slowly, if the bandwidth $h$ used to construct the local linear smoother $\hat{c}(\cdot)$ converges to 0 so slowly that $\nu h \to \infty$ and if the $\theta_i$ become dense in the class of all unit vectors in a half-plane, then $\hat{c} \to c$ in $L^2$.

In principle this discussion refers only to the case where the fractal dimension along transects is identical in all directions. Very similar results may be derived, however, for the

unusual context where there is a unique direction in which the fractal dimension assumes a lower value. In particular, if $c(\cdot)$ is smooth, and $\nu$ is allowed to increase sufficiently slowly, then $c(\cdot)$ is estimated consistently by $\hat{c}(\cdot)$, and $\hat{\alpha}$ is consistent for $\alpha$.

## 6. Application to isotropic data

### 6.1. Description of real data set

The problem treated here arose as part of an experimental study to assess the effect of soil surface roughness on the availability of water for plant growth. A proportion of the rainwater falling onto soil will run off, leaving water retained on the surface to infiltrate the soil. Only this water is accessible by plants. The study was motivated in part by a need to understand how surface roughness relates to the amount of water that is available for plant growth. The very act of precipitation changes the surface's characteristics. The impact causes small craters and dislodges small particles, which are carried by water from one place to another. Therefore, another aim of the study was to analyse the way in which soil surface roughness changes with rainfall.

To obtain the soil surface data the central 512 mm $\times$ 450 mm portion of a 600 mm $\times$ 500 mm dry soil bed was laser scanned. Height averages over circular regions approximately 0.5 mm in diameter were taken at 1 mm intervals along parallel lines 1 mm apart. The soil surface was then subjected to artificial rainfall consisting of raindrops approximately 2.7 mm in diameter, falling from 13 m. Rainfall continued until ponding was evident (free water starts to appear on the surface because the rainfall exceeds infiltration), and the surface was laser scanned again. This procedure was repeated for seven more periods of rainfall, yielding a series of nine images of the soil surface after the following rainfalls (in millimetres): 0.00, 5.30, 10.05, 14.30, 18.55, 22.50, 27.00, 31.25 and 35.50. Details of a closely related experiment, and a variety of images of the resulting soil surfaces, are given by Moran and Vézina (1993). Fig. 5 depicts the last surface for our data (i.e. after 35.50 mm of rainfall) and provides a perspective plot of those data.

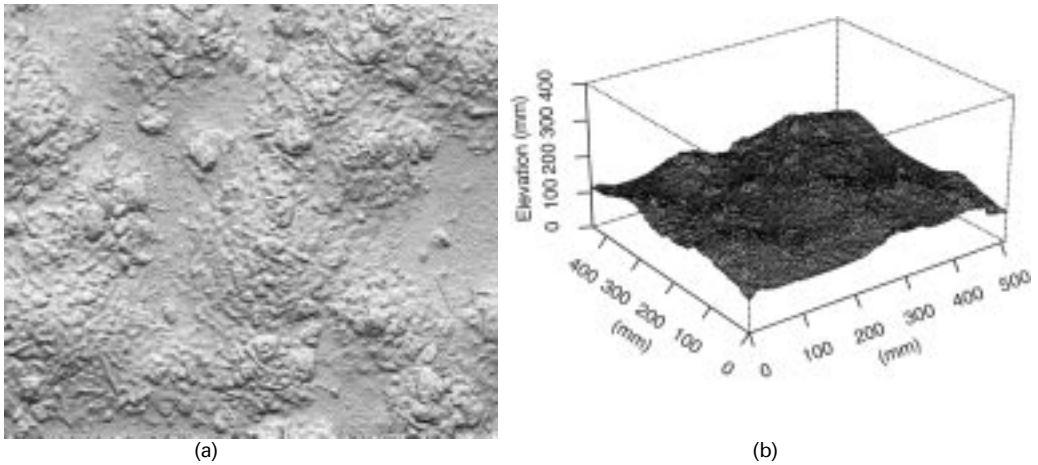


(a) (b)

**Fig. 5.** (a) Artificially shaded view of the soil surface after the maximum amount of simulated rainfall (35.50 mm) and (b) perspective plot of the surface height data used to produce (a): for clarity, only every fourth pixel has been sampled

### *6.2. Point estimation*

Contour plots of $\hat{v}_A$ for the soil surface data (see for example Fig. 6) suggest that the assumption of isotropy is plausible and hence the methods of this section are pertinent. Fig. 7 depicts a scatterplot of the pair $(\log(u), \log\{\hat{v}_I(u)\})$ for one of the data sets, representing the soil surface after 35.50 mm of rain. The line is the OLS regression line corresponding to four points with small lag: $u_1 = 1$; $u_2 = 2^{1/2}$; $u_3 = 2$; $u_4 = 2^{3/2}$.

The estimates of fractal dimension and topothesy for the nine soil data sets are graphed in Fig. 8. Note that the estimated fractal dimension varies relatively little over time, whereas topothesy decreases monotonically after an initial increase. This increase is a consistent feature of many experiments of this type and appears to reflect the 'spattering effect' of a relatively small amount of rainfall on soil surface roughness. The estimates of fractal dimension and topothesy provide soil scientists with summary information on the effect of rainfall on soil surface roughness. Further details of the analysis are available from the first author.

Fitting to the logarithm of the sample variogram has the added advantage, for Gaussian processes, of performing variance stabilization, as indicated numerically by Baczkowski and Mardia (1987).

### *6.3. Interval estimation*

Confidence intervals for $\hat{D}$ and $\hat{c}$, as well as for the statistics introduced in Section 4, are arguably best obtained by using the parametric bootstrap, starting with an appropriate model for the covariance of the process that produced the data. Asymptotic or other non-parametric approaches are hindered by difficulties in estimating the bias and describing the non-normal limit distributions of estimators.

The parametric bootstrap method used to obtain confidence intervals for the soil surface data, as depicted in Fig. 8, was as follows.

*Step 1*: fit a variogram–covariance model to the data. The model used should permit the full range of allowable values for $D$ and $c$. For example, the stable exponential model for

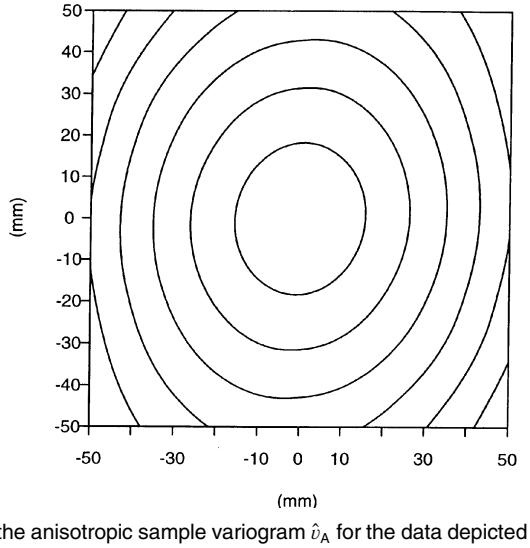


**Fig. 6.** Contour plot of the anisotropic sample variogram $\hat{v}_A$ for the data depicted in Fig. 5(a): the local extremum is a minimum

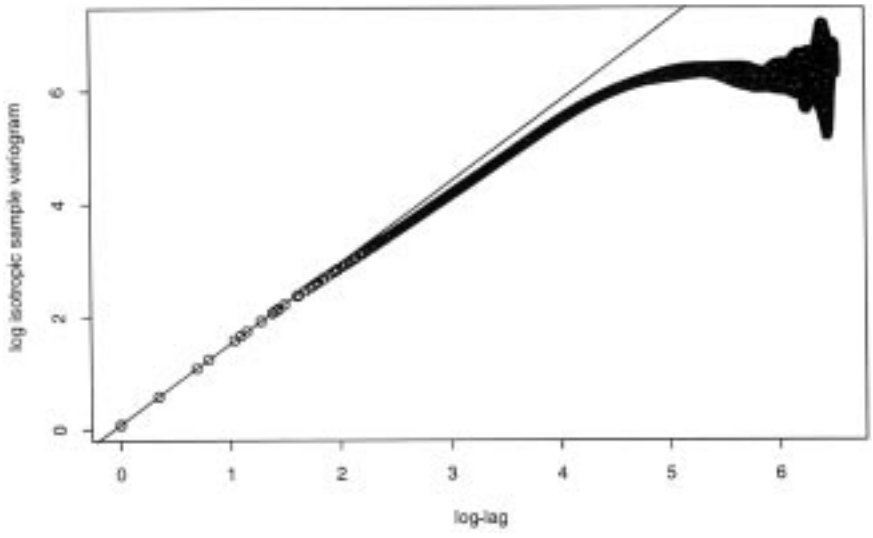


**Fig. 7.** Scatterplot of the logarithm of the isotropic sample variogram $\hat{v}_l$ against log-lag for the data depicted in Fig. 5(a): only lags less than 1000 mm are shown (———, OLS regression through the points with lags 1, $2^{1/2}$, 2 and $2^{3/2}$)

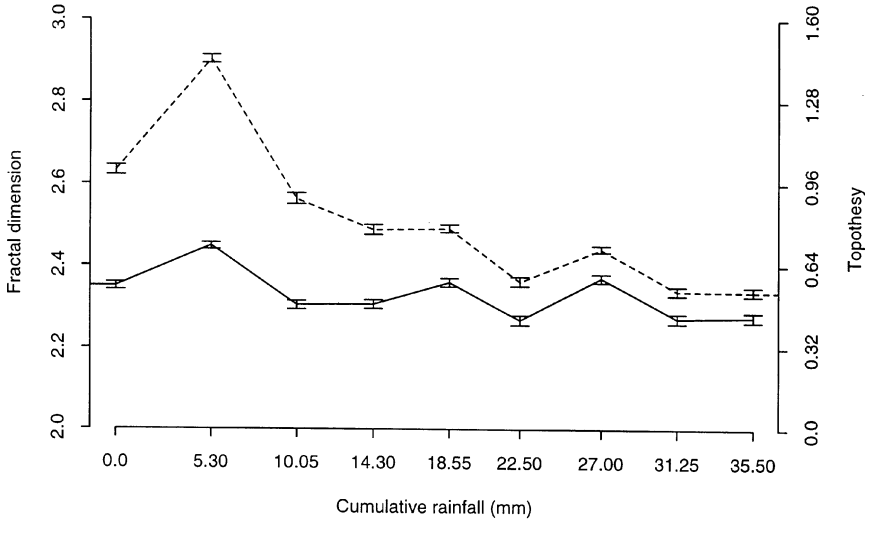


**Fig. 8.** 95% confidence intervals for fractal dimensions (joined by the full line) and topothesies (joined by the broken line) *versus* cumulative rainfall for the soil surface data

the covariance function, $\gamma(t) = c_1 \exp(-c_2\|t\|^{\alpha})$, used in simulations throughout this paper, is appropriate since it is a valid covariance function for all values of $\alpha$ within the interval (0, 2). Here the two parameters $c_1$ and $c_2$ are related to topothesy by $c = c_1 c_2$.

*Step 2*: simulate a number, $B$ say, of realizations of Gaussian random fields with the fitted model as their covariance function. There are many methods for simulating multi-dimensional Gaussian random fields, but one that is particularly useful here, owing to its 'exactness in principle', is due to Wood and Chan (1994). Other methods, such as those

based on the spectrum or on turning bands, approximate the covariance structure. These approximations usually perform worst at the origin, which is precisely where the emphasis of the work in this paper is concentrated.

*Step 3*: for each of the $B$ simulated surfaces, calculate their respective empirical variograms $\hat{v}_{1b}(u)^*$ and use equations (4.2)–(4.4) to obtain $B$ pairs of estimates, $(\hat{D}_b^*, \hat{c}_b^*)$, for the fractal dimension and topothesy.

*Step 4*: use equations similar to equations (4.2)–(4.4), substituting the fitted variogram model from step 1 for $\hat{v}_1(u)$, to obtain expected values $(D^*, c^*)$ for the $(\hat{D}_b^*, \hat{c}_b^*)$ calculated from the simulated data sets. The difference between $(D^*, c^*)$ and the parameter estimates from the original data set $(\hat{D}, \hat{c})$ can be used to correct $(\hat{D}_b^*, \hat{c}_b^*)$ for bias, to obtain $(\tilde{D}_b^*, \tilde{c}_b^*)$.

*Step 5*: let $\{\tilde{D}_{[b]}^*\}$ and $\{\tilde{c}_{[b]}^*\}$ be ordered sets of values taken from the $\tilde{D}_b^*$ and the $\tilde{c}_b^*$ respectively. Marginal $\beta$-level confidence intervals for $D$ and $c$ are then given by $(\tilde{D}_{[2^{-1}\beta B]}^*, \tilde{D}_{[(1-2^{-1}\beta)B]}^*)$ and $(\tilde{c}_{[2^{-1}\beta B]}^*, \tilde{c}_{[(1-2^{-1}\beta)B]}^*)$ respectively. Instead of using step 5 to obtain bootstrap confidence intervals, we could calculate the sample standard deviation of the resampled parameter values $\{\hat{D}_b^*\}$ and $\{\hat{c}_b^*\}$ to obtain estimates of error in point estimation of the parameter values. This approach was used to compute the standard errors in Table 1.

## 7. Application to anisotropic data

### 7.1. Description of real data set

Here the aim was to identify manufacturing processes which produce plastic food wrapping that minimizes the tendency of food to decay. Since decay is hastened by micro-organisms, and smoother wrappers offer less opportunity for those organisms to adhere, an important contribution of the statistical analysis was to compare surfaces in terms of smoothness. The height of the plastic surface, on a microscopic scale, was measured by coating it with a layer of gold just a few molecules thick, and analysing the coated plastic by using a scanning, tunnelling electron microscope. The data from this source were recorded on a 128 × 128 grid, in the form of measurements that were height averages very close to grid point centres. For these data, the pixels were 40 nm × 40 nm. Thus, the second problem involved data on a grid that was many orders of magnitude finer than that for the first.

**Table 1.** Estimated fractal dimensions, average topothesies, levels of anisotropy and maximal roughness orientations for the six plastic food wrapping data sets†

| *Data set* | *Fractal dimension (i)* | *Fractal dimension (ii)* | *Average topothesy* $c_0$ | *Level of anisotropy* $s$ | *Lay* $\psi$ *(rad)* |
|---|---|---|---|---|---|
| (a) | 2.50 | 2.50 | 1.01 | 0.41 | 0.12 |
| | (0.010) | (0.012) | (0.014) | (0.036) | (0.052) |
| (b) | 2.49 | 2.48 | 0.63 | 0.67 | 0.12 |
| | (0.012) | (0.015) | (0.012) | (0.025) | (0.030) |
| (c) | 2.30 | 2.31 | 1.28 | 0.72 | −0.18 |
| | (0.014) | (0.016) | (0.043) | (0.023) | (0.026) |
| (d) | 2.19 | 2.19 | 4.11 | 0.69 | −0.04 |
| | (0.011) | (0.012) | (0.194) | (0.025) | (0.029) |
| (e) | 2.47 | 2.46 | 1.30 | 0.60 | 0.17 |
| | (0.012) | (0.015) | (0.025) | (0.030) | (0.035) |
| (f) | 2.59 | 2.58 | 1.36 | 0.59 | 0.09 |
| | (0.009) | (0.012) | (0.019) | (0.025) | (0.031) |

†The figures in parentheses are bootstrap estimates of the associated standard errors.

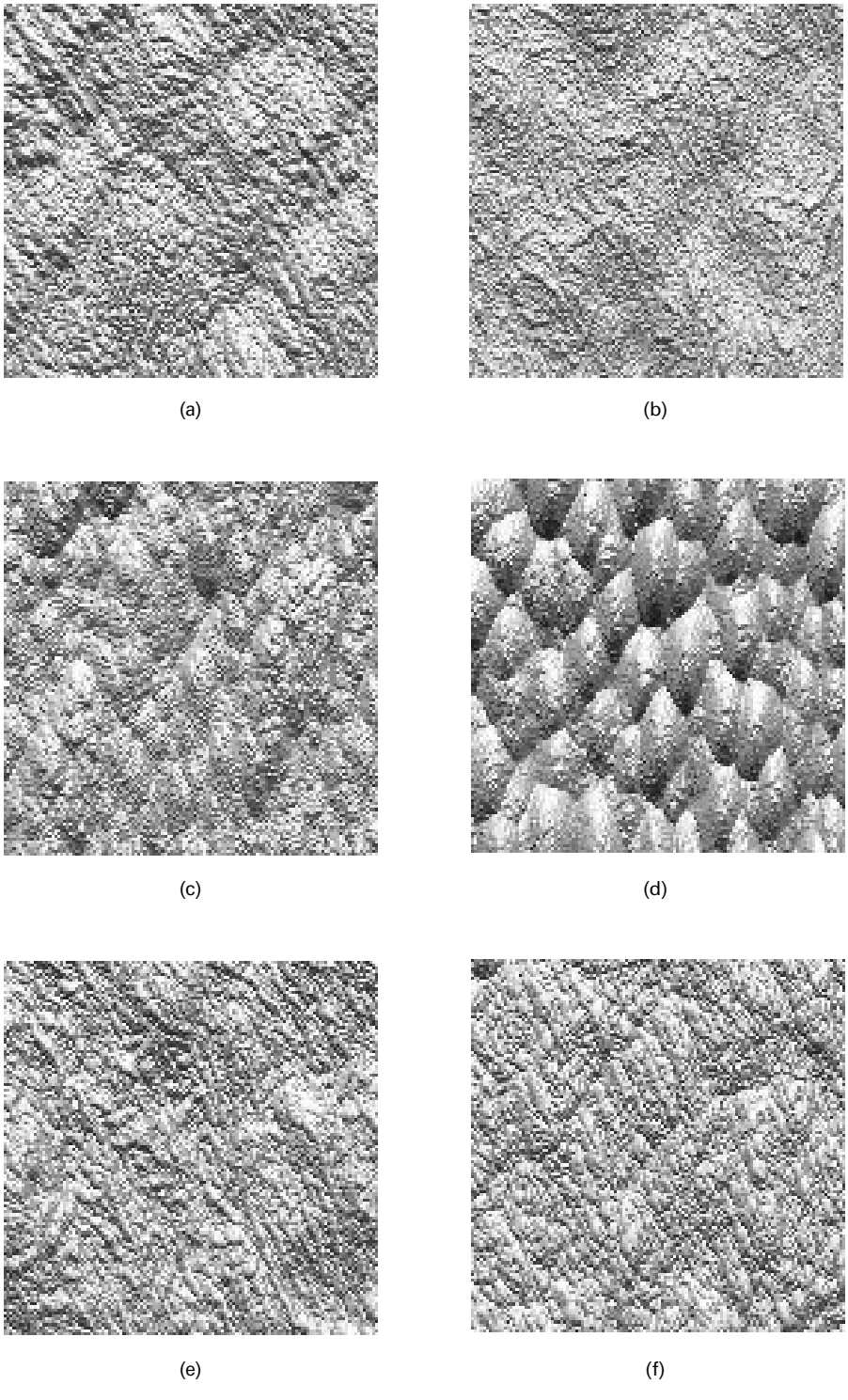


**Fig. 9.** Artificially shaded view of the plastic food wrapping surfaces

Fig. 9 depicts the surfaces of the plastic sheets. The fourth sample is smoother and more regular than the others, although its fractal analysis was not markedly atypical—its fractal properties are on a much finer scale than the bubbles. Fig. 10(a) is a perspective plot of the data represented by Fig. 9(c).

### *7.2. Point estimation*

A high degree of anisotropy is indicated by graphs of $\hat{v}_A$; see for example Fig. 10(b). Fig. 11 is a scatterplot of $\log\{\hat{v}_I(u)\}$ against $\log(u)$ for the third data set, i.e. Fig. 9(c). The full line is the OLS regression line through four points corresponding to $u_1 = 1$, $u_2 = 2^{1/2}$, $u_3 = 2$ and $u_4 = 2^{3/2}$. For each of 24 unit vectors $\omega$, Fig. 12(a) illustrates least squares fits of lines through pairs $(\log(u),\ \log\{\hat{v}_A(u\omega)\})$ with varying $u$, again for the data in Fig. 9(c). The vectors $\omega$ were approximately equally spaced around the circle, subject to the tangents of their orientations being rational. Although the intercepts vary considerably the slopes of the lines are similar, suggesting that the topothesies vary significantly with orientation but the fractal dimensions do not. For comparison, Fig. 12(b) shows analogous lines for the more regular data set, depicted in Fig. 9(d). This surface is smoother, but the evidence of local self-affineness is similar. Formal testing will be addressed in Section 7.4, where we discuss bootstrap methods for these data. Standard errors, in parentheses, were computed as suggested in Section 6.3.

Fractal indices $\hat{\alpha}$ were computed as slopes of OLS regression lines such as that in Fig. 11 and used to compute estimators of fractal dimension by substituting into the formula $\hat{D} = 3 - \frac{1}{2}\hat{\alpha}$; see equation (4.2). Their values are listed in the column labelled 'Fractal dimension (i)' in Table 1.

Contour plots of the sample variogram for the food wrapping data of application 2 were generally elliptical near the origin; see for example Fig. 10(b). We used OLS to fit the

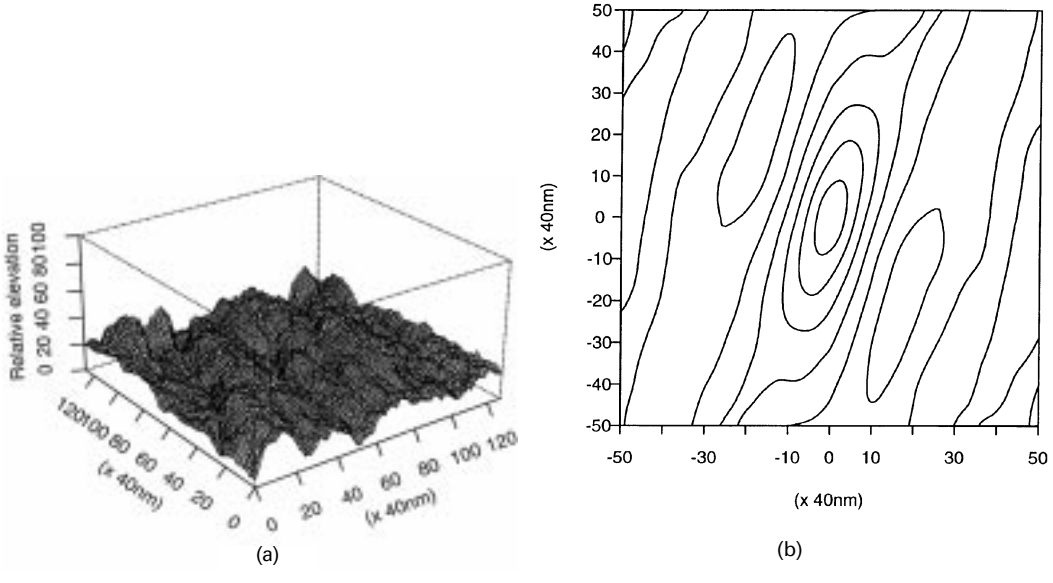


**Fig. 10.** (a) Perspective plot of the surface height data used to produce Fig. 9(c) and (b) contour plot of the anisotropic sample variogram $\hat{v}_A$ for the data depicted in (a): the local extremum is a minimum

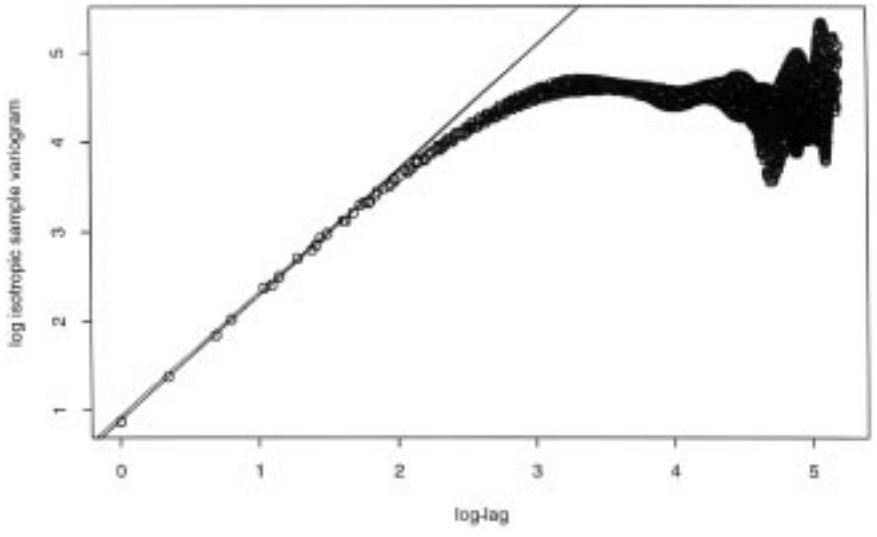


**Fig. 11.** Scatterplot of the logarithm of the isotropic sample variogram $\hat{v}_I$ against log-lag for the data depicted in Fig. 10(a): ———, linear least squares regression through the points with lags 1, $2^{1/2}$, 2 and $2^{3/2}$ (the slope of the dotted line was computed by least squares fitting of the approximate model (4.6))

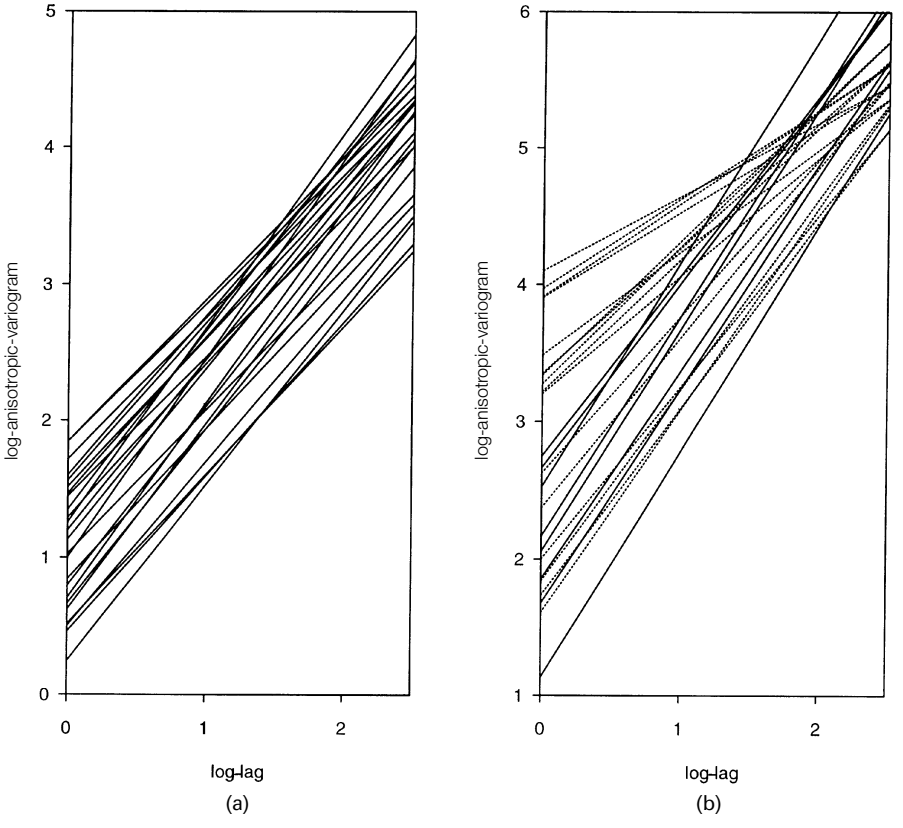


**Fig. 12.** Least squares fits to the scatterplots of the logarithm of the anisotropic sample variogram $\hat{v}_A$, against log-lag for line transects in different directions: (a) for the data depicted in Fig. 10(a); (b) for the data in Fig. 9(d) (·····, fits based on larger lags)

approximate model (4.6) to the logarithm of the anisotropic sample variogram, $\log\{\hat{v}_A(t)\}$, in identical neighbourhoods of the origin. Listed in Table 1 are the corresponding estimates of fractal dimension obtained via equation (4.2) (labelled 'Fractal dimension (ii)', in the third column), $c_0$, $s$ and $\psi$.

The dotted line in Fig. 11 represents the parametrically determined regression line, $\log(\hat{c}_0) + \hat{\alpha}x$, for the data in Fig. 9(c). Fig. 12 depicts plots of $\log(\hat{v}_A)$ for line transect data with 48 different orientations between $-\pi$ and $\pi$. It suggests that the fractal dimension of line transects does not vary with orientation. See also Section 7.3.

Note particularly the difference between Fig. 12(b), and Fig. 2. Only in the former is there a greater tendency for higher slopes to be associated with larger lags. This would not be expected in cases where the dominant fractal dimension in all directions except one was determined by a ruled surface, and so the differences in slope in Fig. 12(b) cannot be explained by that phenomenon. Rather, they appear to be due to the greater bias associated with larger lags.

The $\hat{c}_i$ were calculated from equation (4.5) using those $\theta_i$ for which there existed $u_{ij} \leqslant 5$. Fig. 13 illustrates scatterplots of pairs $(\theta_i, \hat{c}_i)$, together with local linear and parametric smooths of those data. The LOESS statistical package, employing a tricubic kernel and an average bandwidth of $\pi/10$, was used to produce the local linear smooth. (The amount of smoothing needed to produce graphs such as Fig. 13 is usually easy to determine by eye, since the points on the curve are themselves estimates and so have relatively little noise.) The parametric smooth was obtained by using the asymptotic model (4.6). Note that both curves differ from a pure sinusoid in that the curvature of the crests is less than that of the troughs. Further details of the analysis are available from the first author.

The fourth data set (the markedly regular data) has lower fractal dimension than the others and higher average topothesy. The last column of Table 1 suggests that these data are at least as amenable as the others to analysis by our methods. This surface may show evidence of two fractal dimensions at different lags, or scales: see Fig. 12(b), where the lines corresponding to larger lags (the dotted lines) have lesser slope. However, this is probably due, at least in part,

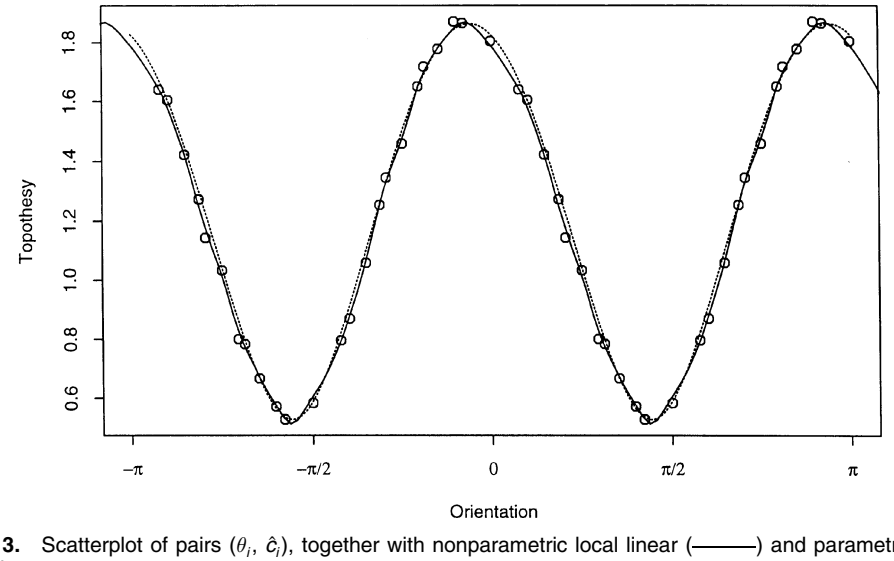


**Fig. 13.** Scatterplot of pairs $(\theta_i, \hat{c}_i)$, together with nonparametric local linear (———) and parametric (·····) smooths

to greater error in the estimation of the variogram from which those lines were constructed. For larger lags, fewer points, and hence less information, were used.

From the material scientists' point of view, the estimates of fractal dimension provide criteria for ranking plastic food wrapping surfaces in order of roughness. This provides them with information for determining the manufacturing process that produces food wrapping with the most desirable properties.

### 7.3. Hypothesis testing

We give here a bootstrap method, similar to that for interval estimation in Section 6.3, for comparing roughness parameters between surfaces. First we provide an informal description of a method for testing the hypothesis that two surfaces have a common fractal dimension.

*Step 1*: fit a variogram–covariance model to the data. The model used should permit the whole range of allowable values for each of the anisotropic roughness parameters. For the parameter under investigation, pool the parameter estimates obtained from the two surfaces, and substitute the pooled estimate for the values in the models from which we shall resample. For example, to compare the fractal dimensions of two anisotropic surfaces, we might take the average of their estimated fractal indices and substitute it for the original fitted values in their respective fitted models, leaving all other parameter estimates the same.
*Step 2*: from the modified models for each surface, simulate a number, $B$ say, of realizations of Gaussian random fields. These simulations will then be conducted under the null hypothesis that the surfaces have similar underlying parameter values.
*Step 3*: for each of the $2B$ simulated surfaces, calculate their respective empirical variograms $\hat{v}_{\mathrm{A}b}(u)^*$ and fit model (4.6), to obtain $B$ sets of parameter estimates from each model.
*Step 4*: for the parameter in question, calculate the absolute difference of its estimated values from every combination of pairs of the simulated surfaces, one from either model, to obtain a bootstrap distribution. Then compare the absolute difference of the parameter's estimated values for the two real surfaces. Compare this statistic with the bootstrap statistics. The proportion of bootstrap statistics that exceed the actual statistic yields an approximate $p$-value.

The plastic food wrapping data sets were manufactured by two slightly different processes, sets (a), (c) and (e) by one process and sets (b), (d) and (f) by the other. Successive pairs of data sets had similar input parameters for each process. One of the aims of the experiment was to determine whether the roughness properties of surfaces manufactured by the first process were different from those for surfaces manufactured by the second process, for a range of input parameter values.

Table 2 contains results from bootstrap hypothesis tests for a common fractal dimension. As can be concluded from Table 2, the difference in fractal dimension for the first pair of surfaces is possibly caused by stochastic error, whereas differences for the other pairs are most likely not due to stochastic error.

## 8. Conclusions

We have shown that, for spatial data, the fractal dimension of line transects across a surface has only limited freedom to vary with orientation. For even a highly anisotropic stationary

**Table 2.** Test statistics and associated *p*-values for parametric bootstrap tests for a common fractal dimension between successive pairs of the six plastic food wrapping data sets

| *Data sets* | *Statistic* | *p-value* |
|---|---|---|
| (a) and (b) | 0.016 | 0.637 |
| (c) and (d) | 0.133 | 0.000 |
| (e) and (f) | 0.125 | 0.000 |



random field, the fractal dimension must be the same in all directions except possibly one, where it may assume a lower value. This means that an adequate account of the way in which surface roughness changes with orientation must rely significantly on the scale. We have suggested a periodic function definition of topothesy for describing scale and discussed parametric (e.g. sinusoid-based), semiparametric and nonparametric (e.g. kernel-based) methods for estimating the function. Theoretical and numerical properties of our estimators have been described, and the estimators have been shown to perform well for even non-replicated data.

Together, fractal dimension and topothesy describe all first-order aspects of the behaviour of the covariance function of a stationary random field at the origin. In this sense, fractal properties may be said to capture the essence of roughness characteristics. However, higher order terms describing the fluctuations of covariance may also be important, depending on the application. For example, this is the case if a surface may plausibly be modelled as a sum of ruled surfaces, as in our example 1. As we noted there, fractal methods cannot capture more than the two most dominant components.

## Acknowledgements

Helpful comments from and discussions with M. Berman, G. Chan, A. G. Constantine, N. I. Fisher, P. N. Jones and A. T. A. Wood are gratefully acknowledged. Thanks are also due to Dr C. Moran and Mr J. Taylor from CSIRO Land and Water, and Dr H. Griesser and Mr T. Gengenbach from CSIRO Molecular Science, for providing the real data sets which motivated the work. The comments of four referees and an editor have also proved particularly helpful.

## Appendix A: Outline proof of theorem 2

Let $\Sigma_m$ denote summation over $(i_m, j_m, k_m, l_m) \in \mathcal{S}_1(u)$, for $m = 1, 2$. In this notation,

$$\mathrm{var}\{\hat{v}_1(u)\} = N_1(u)^{-2} \sum_1 \sum_2 T(i_1, j_1, k_1, l_1, i_2, j_2, k_2, l_2),$$

where

$$T(i_1, j_1, k_1, l_1, i_2, j_2, k_2, l_2) = E[\{X(t_1) - X(t_1 + t_2)\}^2 \{X(t_3) - X(0)\}^2],$$

$t_1 = t_{i_1 j_1} - t_{k_2 l_2}$, $t_2 = t_{k_1 l_1} - t_{i_1 j_1}$ and $t_3 = t_{i_2 j_2} - t_{k_2 l_2}$. It suffices to show that

$$\mathrm{var}\{\hat{v}_1(u)/v(u)\} = O(n^{2\alpha-4} \lambda_n^2). \tag{A.1}$$

Since $X$ is Gaussian then

$$T(i_1, j_1, k_1, l_1, i_2, j_2, k_2, l_2) = 2\{\gamma(t_1) + \gamma(t_1 + t_2 - t_3) - \gamma(t_1 - t_3) - \gamma(t_1 + t_2)\}^2. \quad \text{(A.2)}$$

Let $\Sigma_3$ and $\Sigma_4$ denote summation over $(i_1, j_1, k_1, l_1)$, $(i_2, j_2, k_2, l_2)$ satisfying $(i_m, j_m, k_m, l_m) \in \mathcal{S}_1(u)$ for $m = 1, 2$ and $\|t_1\| \leqslant 3u$ and $\|t_1\| > 3u$ respectively. Define

$$S_j = \textstyle\sum_{2+j} T(i_1, j_1, k_1, l_1, i_2, j_2, k_2, l_2)$$

for $j = 1, 2$. In the case of $S_1$ there are $O(n^2)$ summands, and we bound them using the identity (A.2):

$$\begin{aligned} |T(i_1, j_1, k_1, l_1, i_2, j_2, k_2, l_2)| &\leqslant 2\{|v(t_1)| + |v(t_1 + t_2 - t_3)| + |v(t_1 - t_3)| + |v(t_1 + t_2)|\}^2 \\ &\leqslant C_1 u^{2\alpha}, \end{aligned}$$

where $C_1, C_2, \ldots$ denote generic positive constants. Hence, $|S_1| \leqslant C_2 n^2 u^{2\alpha} \leqslant C_3 n^{2-2\alpha}$, since $u = O(n^{-1})$. In the case of $S_2$ there are $O(n^4)$ summands, each of which we bound using a Taylor expansion argument which requires conditions (5.5) and (5.6). Arguing thus we obtain first that

$$T(i_1, j_1, k_1, l_1, i_2, j_2, k_2, l_2) \leqslant C_4(\|t_1\|^{\alpha-2})^2,$$

and thence

$$\begin{aligned} |S_2| &\leqslant C_5 n^4 \textstyle\sum_4 \|t_1\|^{2(\alpha-2)} \\ &\leqslant C_6 n^{-4} n^{-2(\alpha-2)} n^2 \int_1^n \mathrm{d}x_1 \int_0^n (x_1 + x_2)^{2(\alpha-2)} \, \mathrm{d}x_2 = O(\lambda_n^2). \end{aligned}$$

Therefore, $\mathrm{var}\{\hat{v}_1(u)\} = N_1(u)^{-2}(S_1 + S_2) = O(n^{-4}\lambda_n^2)$, from which follows the desired result (A.1).

## References


Adler, R. J. (1981) *The Geometry of Random Fields*. New York: Wiley.

Baczkowski, A. J. and Mardia, K. V. (1987) Approximate lognormality of the sample semi-variogram under a Gaussian process. *Communs Statist. Simuln*, **16**, 571–585.

Banjeri, K. (1988) Quantitative fractography: a modern perspective. *Metall. Trans.* A, **19**, 961–971.

Barnsley, M. (1988) *Fractals Everywhere*. New York: Academic Press.

Berry, M. V. (1979) Diffractals. *J. Phys.* A, **12**, 781.

Berry, M. V. and Hannay, J. H. (1978) Topography of random surfaces. *Nature*, **273**, 573.

Berry, M. V. and Lewis, Z. V. (1980) On the Weirstrass–Mandelbrot fractal function. *Proc. R. Soc. Lond.* A, **370**, 459–484.

Chan, G., Hall, P. and Poskitt, D. S. (1995) Periodogram-based estimators of fractal properties. *Ann. Statist.*, **23**, 1684–1711.

Constantine, A. G. and Hall, P. (1994) Characterizing surface smoothness via estimation of effective fractal dimension. *J. R. Statist. Soc.* B, **56**, 97–113.

Cramér, H. and Leadbetter, M. R. (1963) *Stationary and Related Stochastic Processes*. New York: Wiley.

Cressie, N. A. C. (1991) *Statistics for Spatial Data*. New York: Wiley.

Cutler, C. D. (1991) Some results on the behaviour and estimation of fractal dimensions of distributions on attractors. *J. Statist. Phys.*, **62**, 651–708.

Dauskardt, R. H., Habensk, F. and Ritchie, A. (1990) On the interpretation of the fractal character of fractal surface. *Acta Metall.*, **38**, 143–159.

Davies, S. (1998) The stochastic analysis of surface roughness—a fractal-based approach. *PhD Thesis*. Australian National University, Canberra.

Dubuc, B., Quiniou, J. F., Roques-Carmes, C., Tricot, C. and Zucker, S. W. (1989a) Evaluating the fractal dimension of profiles. *Phys. Rev.* A, **39**, 1500–1512.

Dubuc, B., Zucker, S. W., Tricot, C., Quiniou, J. F. and Wehbi, D. (1989b) Evaluating the fractal dimension of surfaces. *Proc. R. Soc. Lond.* A, **25**, 113–127.

Falconer, K. J. (1985) *The Geometry of Fractal Sets*. Cambridge: Cambridge University Press.

Fan, J. (1993) Local linear regression smoothers and their minimax efficiencies. *Ann. Statist.*, **21**, 196–216.

Fedderer, H. (1969) *Geometric Measure Theory*. Berlin: Springer.

Feuerverger, A., Hall, P. and Wood, A. T. A. (1994) Estimation of fractal index and fractal dimension of a Gaussian process by counting the number of level crossings. *J. Time Ser. Anal.*, **15**, 587–606.

Gilbertson, L. N. and Zipp, R. D. (1981) *Fractography and Materials Science*. Philadelphia: American Society for Testing and Materials.

Greenwood, J. A. (1984) Unified theory of surface roughness. *Proc. R. Soc. Lond.* A, **393**, 133–157.

Hall, P. and Davies, S. (1995) On direction-invariance of fractal dimension on a surface. *Appl. Phys.* A, **60**, 271–274.
Hall, P. and Roy, R. (1994) On the relationship between fractal dimension and fractal index for stationary stochastic processes. *Ann. Appl. Probab.*, **4**, 241–253.
Hall, P. and Wood, A. T. A. (1993) On the performance of box-counting estimators of fractal dimension. *Biometrika*, **80**, 246–252.
Hastie, T. and Loader, C. (1993) Local regression: automatic kernel carpentry. *Statist. Sci.*, **8**, 120–143.
Hsü, K. J. and Hsü, A. J. (1990) Fractal geometry of music. *Proc. Natn. Acad. Sci. USA*, **87**, 938–941.
Jain, P. S. (1986) Fractal dimensions of clouds around Madras. *Mausam*, **40**, 311–316.
Kent, J. T. and Wood, A. T. A. (1997) Estimating the fractal dimension of a locally self-similar Gaussian process by using increments. *J. R. Statist. Soc.* B, **59**, 679–699.
Lewin, R. (1991) The fractal structure of music. *New Scient.*, **130**, no. 1767, 15.
Ling, F. F. (1987) Scaling law for contoured length of engineering surfaces. *J. Appl. Phys.*, **62**, 2570–2572.
———(1989) The possible role of fractal geometry in tribology. *Tribol. Trans.*, **32**, 497–505.
Lo, T., Leung, H., Litva, J. and Haykin, S. (1993) Fractal characterisation of sea-scattered signals and detection of sea surface targets. *IEE Proc.* F, **140**, 243–250.
Mandelbrot, B. B. (1982) *The Fractal Geometry of Nature*. San Francisco: Freeman.
———(1985) Self-affine fractals and fractal dimension. *Phys. Scr.*, **32**, 257–260.
Mandelbrot, B. B., Passoja, D. E. and Paullay, A. J. (1982) Fractal character of fracture surfaces of metals. *Nature*, **308**, 721–722.
Marstrand, J. M. (1954) Some fundamental geometrical properties of plane sets of fractal dimensions. *Proc. Lond. Math. Soc.*, **4**, 257–302.
Massopust, P. R. (1994) *Fractal Functions, Fractal Surfaces, and Wavelets*. San Diego: Academic Press.
Matthews, D. T. (1998) On fractal dimension and its application. *PhD Thesis*. Australian National University, Canberra.
Mattila, P. (1985) On the Hausdorff dimension and capacities of intersections of sets in *n*-space. *Acta Math.*, **152**, 77–105.
Milne, B. T. (1991a) The utility of fractal geometry in landscape design. *Lands. Urb. Planng*, **21**, 81–90.
———(1991b) Lessons from applying fractal models to landscape patterns. In *Quantitative Methods in Landscape Ecology* (eds M. G. Turner and R. H. Gardner), pp. 199–235. New York: Springer.
Moran, J. and Vézina, G. (1993) Visualizing soil surfaces and crop residues. *IEEE Comput. Graph. Appl.*, Mar., 40–47.
Morrison, A. I. and Srokosz, M. A. (1993) Estimating the fractal dimension of the sea surface: a first attempt. *Ann. Geophys.*, **11**, 648–658.
Ogata, Y. and Katsura, K. (1991) Maximum likelihood estimates of the fractal dimension for spatial patterns. *Biometrika*, **78**, 463–474.
Passoja, D. E. and Amborski, D. J. (1978) Fractal profile analysis by Fourier transform methods. *Microstruct. Sci.*, **6**, 143–148.
Passoja, D. E. and Psioda, D. J. (1981) Fourier transformation techniques — fracture and fatigue. In *Fractography and Materials Science* (eds L. N. Gilbertson and R. D. Zipp), pp. 335–386. Philadelphia: American Society for Testing and Materials.
Rigaut, J. P. (1988) Automated segmentation by mathematical morphology and fractal geometry. *J. Microsc.*, **150**, 21–30.
Rosenblatt, M. (1961) Independence and dependence. In *Proc. 4th Berkeley Symp. Mathematical Statistics and Probability* (ed. J. Neyman), pp. 411–433. Berkeley: University of California Press.
Sayles, R. S. and Thomas, T. R. (1977) The spatial representation of surface roughness by means of the structure function: a practical alternative to correlation. *Wear*, **42**, 263–276.
———(1978) Surface topography as a nonstationary random process. *Nature*, **271**, 431–434.
Serinko, R. J. (1994) A consistent approach to least squares estimation of correlation dimension in weak Bernoulli dynamical systems. *Ann. Appl. Probab.*, **4**, 1234–1254.
Stout, K. J., Sullivan, P. J., Dong, W. P., Mainsah, E., Luo, N., Mathia, T. and Zahouani, H. (1993) The development of methods for the characterisation of roughness in three dimensions. *Publication EUR 15178*. Commission of the European Communities Dissemination of Scientific and Technical Knowledge Unit, Directorate–General for Information Technologies and Industries, and Telecommunications, Luxembourg.
Stoyan, D. and Stoyan, H. (1994) *Fractals, Random Shapes and Point Fields*. Chichester: Wiley.
Taqqu, M. S. (1975) Weak convergence to fractional Brownian motion and to the Rosenblatt process. *Z. Wahrsch. Ver. Geb.*, **31**, 287–302.
Taylor, C. C. and Taylor, S. J. (1991) Estimating the dimension of a fractal. *J. R. Statist. Soc.* B, **53**, 353–364.
Thomas, T. R. (1982) *Rough Surfaces*. London: Longman.
Thomas, T. R. and Thomas, A. P. (1988) Fractals and engineering surface roughness. *Surf. Topogr.*, **1**, 143–152.
Underwood, E. E. and Banjeri, K. (1986) Fractals in fractography. *Mater. Sci. Engng*, **80**, 1–14.
Wang, Y. (1997) Fractal function estimation via wavelet shrinkage. *J. R. Statist. Soc.* B, **59**, 603–613.
Whitehouse, D. and Phillips, M. J. (1982) Two-dimensional discrete properties of random surfaces. *Phil. Trans. R. Soc. Lond.* A, **305**, 441–468.
Wood, A. T. A. and Chan, G. (1994) Simulation of stationary Gaussian processes in $[0, 1]^d$. *J. Comput. Graph. Statist.*, **3**, 409–432.

## Discussion on the paper by Davies and Hall

**Charles Taylor** (*University of Leeds*)

I would like to congratulate Steve Davies and Peter Hall on a most interesting paper which has — for me at least — just the right balance of theoretical results, applications and data analysis. These ingredients are nicely woven together. In starting off the discussion, I would like to focus on three areas which arise from the paper and to ask various questions which I believe to be of interest.

First, on resolution issues, as we have heard, the notion of fractal dimension has evolved in pure mathematics and formal definitions were given in terms of infinitesimal limits. In recent years the study of fractals has been transformed from an interesting mathematical curiosity to a fashionable tool of scientific thinking. Their popularity is I believe due, to a large extent, to the work of Mandelbrot (1977, 1982). Within these books there are many pictures which show that very realistic scenes can be obtained by simulations of fractals with appropriate parameters. As statisticians, it is natural to consider whether, starting from scenes such as these, the fractal dimension can be estimated from the data.

One of the ways of calculating the fractal dimension of a line is to measure the *length* of the line by using a pair of dividers set to a prescribed opening. The length can be approximated by counting the number of steps, and multiplying this by the step length. The total length is then a non-increasing function of the step length. Again, fractal-like behaviour can be observed for real physical phenomena. With tongue in cheek, I offer the example of Richardson (1961), who plotted the logarithm of length of various land–land and land–sea boundaries as a function of the logarithm of the step length. If we abandon our statistical senses, and claim that these physical phenomena are true fractals, then with appropriate extrapolation it can be seen that the west coast of Britain is longer than the entire coastline of Australia! Our theory suggests that this occurs if the step length is less than 0.03 mm, at which point the grains of sand — and the gaps between them — will have a dominating effect.

I have several questions which arise from this. As the possibility of increasingly finer resolutions becomes available, should we not be developing methods which fit piecewise linear lines (with each line relevant to a particular range of scales) to these log–log-plots rather than just estimating the limiting slope? Discriminating between surfaces could be made easier if more information were used.

Incidentally, the authors propose to use four small scales in the estimation of the slope (steps of length 1 and 2 in the vertical and horizontal directions, and of length $\sqrt{2}$ and $2\sqrt{2}$ diagonally). Why did they not use $\sqrt{5}$?

My second point concerns the fitting of straight lines to points. In Section 5.1 the authors correctly point out that estimates of the variogram exhibit high correlation between values at neighbouring lags. This being the case, why use *ordinary* least squares in fitting rather than *generalized* or perhaps just *weighted* least squares?

Several years ago, Taylor and Taylor (1991) used the method of *box counting*, rather than the variogram, to estimate fractal dimension. In the case of a fractal, a plot of log(number of boxes 'hit') *versus* log(box size) is nearly linear, but typical residual plots showed strong correlation. Incidentally, I would have been interested to see some residual plots in the paper. Davies and Hall assume (in their bootstrap simulations) that the data are like realizations of a Gaussian random field. It should be possible to use the Fourier inversion method of Davis and Borgman (1979) to calculate the exact sampling distribution of the variogram. See also Cressie (1985) who fitted variogram models by generalized least squares. In any case, one might ask: what does the empirical correlation matrix of the (log-) variogram estimates from such realizations look like? My (again limited) experience of both simulated fractional Brownian motion and a simulated stable process suggests that the correlations should be taken account of.

To some extent the practice of using the bootstrap should take care of these points, but it would nevertheless be interesting to try generalized least squares and to compare the results.

One wonders whether it might be possible to check whether the Gaussian model is appropriate for these data. Alternatively, would it be possible to use some sort of nonparametric bootstrap which resamples the data and makes no distributional assumptions? I can only feel that the confidence intervals shown in Fig. 8 are too small (this could arise if the data were not Gaussian, or not stationary, or if there were outliers etc.). Each point is based on just one image, and I wonder whether these apparently significant changes over time have a physical explanation.

Finally, I turn to questions of inference which are raised in Section 7.3. The main result of this paper is that the fractal dimension of line transects across a *stationary* fractal surface must be the same in all directions except possibly one. This is an interesting, and I think useful, result. It would be nice if we could apply formal statistical tests which would confirm the hypothesis of stationarity and/or isotropy.

The last line of Section 3 states that 'Fig. 2 shows that the variation of fractal dimension is evident empirically'. This begs the question: can we *test* for stationarity or isotropy? The level $s$ of anisotropy shown in Table 1 indicates that this can be done, but it would be reassuring to know whether the significance level of the test was validated by checking with some simulated data. Also, it would be comforting to see whether the same test applied to the soil surface data yielded values of $s$ that are suitably close to 0.

Also, what about estimates of lay, the direction in which the topothesy is largest? Surely if there is only one direction in which the fractal dimension differs — assuming that we could find it — it should be lined up with the pixel structure of the data. Presumably there is a problem in estimating directions which are very close to the line of the pixels. In any case the estimates of the last column of Table 1 should be the same; are the fluctuations not too large compared with the standard errors for this conclusion to hold? For the anisotropic data, the fractal dimension differs only in the direction orthogonal to $\psi$. Can you estimate the fractal dimension in this particular direction and test whether it is different?

Davies and Hall are tackling a very interesting problem, and I am sure that this paper will stimulate plenty of further work in this area. In conclusion I have much pleasure in proposing a vote of thanks to Steve Davies and Peter Hall for a thought-provoking paper.

**B. D. Ripley** (*University of Oxford*)

One of the traditions of the Society is that the seconder may act as an 'opponent', a role that I feel comfortable with, as when I first encountered fractal methods for surfaces nearly 20 years ago I did not believe in them, and I still do not. In reviewing what this paper might have to say about similar examples I have encountered, I found that some of the unemphasized assumptions were critical.

Let me start at the beginning. I was misled by the title and summary. This paper is not about surface roughness; it is about the roughness of a postulated generative process, more precisely about the second-order properties of that process. Now second-order properties characterize Gaussian processes but not others, and I wondered whether methods that are appropriate for Gaussian processes were necessarily appropriate for more realistic generative processes. The issue is not whether the theory holds for non-Gaussian processes but whether the appropriate statistics have been collected.

Sections 6 and 7 are entitled 'Application to (an)isotropic data'. I submit that it is the process not the data that is isotropic. This may sound pedantic, but the difference can be important. (I recalled that I had said this before in a similar role: Ripley (1985).) Stationarity (including isotropy) is an assumption about what might have happened but did not. The generative process in the food wrapping example is only anisotropic if the specimens are always aligned in some fixed way, *but* the measurement process in both the authors' examples is anisotropic (it involves a square grid). This begs the question: is the anisotropy found in Table 1 a function of the material or of the measurement? Rotating the specimen and seeing how the estimated $\psi$ changes would be a good check on this and the estimated standard errors.

My first encounter with fractals in this context was when I received a letter from Mandelbrot about Fig. 1.3 of Ripley (1981) which he suggested had a fractal structure. This was a cross-section of a small piece of rock, and my answer was that there were only two scales of interest: those of crude oil and water molecules. I have heard many talks at oil-industry meetings since about fractal methods, but with few successful applications. The explanation given in the paper for the motivation for the food wrapping example (which differs from that in the oral presentation) is about organisms adhering to the wrapping: surely that has a crucial scale.

The next example that I found in my files was from Appleyard *et al*. (1985). This trumps the gold-plated food wrapping by being of *platinum*-coated walls of human muscle cells. Again there are two crucial scales corresponding to 'bumps' of two different proteins. That picture is shaded like those of Figs 5 and 9, and I remembered that rotating it by 180° gives the impression of viewing from the reverse side. Try this on Fig. 9. This is a version of an old trick for time series: samples from Gaussian series look the same when reversed and with a sign change. Covariance properties cannot reveal the differences that I see on rotating Fig. 9, and this begs the question of whether the roughness of the peaks or of the troughs is important in the application.

Just above equation (4.6) we have 'an elliptically contoured variogram' which I think means ellipses with common axes; if so it is what in my experience is much more commonly called 'geometric anisotropy'. This led me to wonder whether the axes could change appreciably with scale: they can (Ripley (1981), Fig. 6.12). That figure reminded me that spectral methods can be instructive for

regularly sampled spatial surfaces, and *that* took me back to Ford (1976). David Ford studied the top of the canopy of a 120 m × 36 m block of a pine forest at 1-m spacing. This is a spatial surface where excursions in only one direction are important, and again the direction of apparent anisotropy varies with scale. This example relates to the discussion at the end of Section 2. Fractal methods are concerned with the limit at small scales: in theory we apply the behaviour of the surfaces of individual pine-needles to the canopy!

Asymptotics in spatial processes can be problematic: there are many ways to infinity (Ripley (1988), pages 2–3). The issue is into which series of problems to embed the observed one. It was not clear to me that this is adequately addressed: should not the points $(u_i)$ depend on $n$ in the asymptotics to correspond to the data analysis procedure used in Fig. 7?

I have reservations about whether the assumptions made in this paper are widely applicable, even to its own examples, but I found it stimulating (and nostalgic) and it is a great pleasure to second the vote of thanks.

The vote of thanks was passed by acclamation.

**Andrew Wood** (*University of Bath*) **and Grace Chan** (*University of New South Wales, Kensington*)
We mention some alternative estimators of fractal dimension. In the case $d = 1$ (which corresponds to line transect sampling), Kent and Wood (1997) considered two ways of modifying the traditional variogram estimator studied by Constantine and Hall (1994):

(a) base the variogram on *second-order* differences (equivalently, first-order increments) of the form $X_{t+h} + X_{t-h} - 2X_t$ rather than *first-order* differences (equivalently, zeroth-order increments) $X_{t+h} - X_t$;
(b) use *generalized least squares* (GLS) rather than *ordinary least squares* (OLS) when estimating $\alpha$ via the log–log-relationship (see equation (4.1)). A suitable weight matrix can be constructed by using the Gaussian assumption and the assumption concerning the behaviour of the covariance function at the origin.

The use of second-order differences leads to estimators with asymptotic variance of order $N^{-1}$ and a normal limit distribution, for all $\alpha \in (0, 2)$. However, with typical sample sizes, estimators based on (a) and OLS performed less well than the traditional estimator, even though for smoother surfaces the theory suggested otherwise; see Kent and Wood (1997). However, GLS improved the finite sample performance, which relates to a point by Charles Taylor.

Modifications (a) and (b) can also be used when $d = 2$, as in the paper; see Chan and Wood (1997). The two-dimensional analogue of taking second differences which seems to work best is what we call the 'square increment', described loosely by the expression $X_{s+h,t+k} + X_{s,t} - X_{s,t+k} - X_{s+h,t}$. We constructed a variogram using differences of this kind, and the resulting estimators of $\alpha$ have 'standard' asymptotics, in the above sense. We also used GLS rather than OLS, but the calculation of a suitable weight matrix (which we derived from the 'elliptical' model for the covariance function) is more complex than when $d = 1$.

When $d = 1$, modifications (a) and (b) are 'variations on a theme'. However, for $d = 2$, there are quite substantial structural differences between the estimators considered by Chan and Wood and those in the paper. It is therefore of interest to compare numerical results for the plastic wrapper data sets.

**Table 3.** Chan and Wood (1997) estimates for the plastic wrapping data

| *Wrapping* | *Isotropy assumed* | | *Elliptical model* | | | |
|---|---|---|---|---|---|---|
| | $\hat{D}_1$ | *Standard error* | $\hat{D}_2$ | *Standard error* | $\hat{s}$ | $\hat{\psi}$ |
| 1 | 2.45 | 0.011 | 2.44 | 0.009 | 0.46 | 0.26 |
| 2 | 2.64 | 0.010 | 2.63 | 0.009 | 0.57 | 0.14 |
| 3 | 2.33 | 0.011 | 2.39 | 0.018 | 0.77 | −0.10 |
| 4 | 2.03 | 0.012 | 2.12 | 0.023 | 0.97 | −0.04 |
| 5 | 2.45 | 0.011 | 2.44 | 0.009 | 0.60 | 0.23 |
| 6 | 2.56 | 0.010 | 2.55 | 0.008 | 0.72 | 0.09 |

The estimates and standard errors in Table 1 and those in Table 3 are quite similar, with the possible exception of the fourth data set. Our standard errors were obtained from the weight matrix, whereas those in the paper were obtained using a parametric bootstrap method. It is reassuring that the numerical results are so similar.

We conclude with two brief comments. First, both sets of standard errors are rather small. To what extent do they reflect the true variability of the estimates? Second, it seems reasonable to hope that the 'bad' asymptotics indicated in theorem 2 for smoother surfaces will not lead to serious problems in practice; see Sections 5 and 6 in Kent and Wood (1997) for relevant discussion when $d = 1$.

**Jianqing Fan** (*University of California, Los Angeles*) **and Qiwei Yao** (*University of Kent, Canterbury*)

The authors are to be congratulated for important contributions to the beautiful theory and elegant methods of estimating fractal dimensions. We welcome the opportunity to provide alternative methods for estimating fractal indices and inference tools.

*Estimation in isotropic case*

Davies and Hall's method is based on fitting a local linear model to the approximate model (4.1) for small $\|t\|$. A more direct approach is based on the fact that

$$\frac{\{X(t) - X(u)\}^2}{2\,\gamma(0) - 2\,\gamma(\|t - u\|)} \sim \chi_1^2$$

for a stationary Gaussian process. Let $a_0 = E\{\log(Z^2)\} \approx -1.27$, where $Z \sim N(0, 1)$. Then, we can now directly use the approximate model

$$\log\{X(t_{ij}) - X(t_{kl})\}^2 - a_0 = \log(2c) + \alpha\ \log(\|t_{ij} - t_{kl}\|) + \text{noise}$$

for $\|t_{ij} - t_{kl}\| \leqslant r$, where $r$ is a prescribed constant determining the size of the local neighbourhood. This method is also applicable to the case where data are collected at irregular design points. It provides a useful alternative method for estimating fractal dimensions.

*Anisotropy and partially linear models*

In Section 4.2, the authors propose to use procedure (4.3) for estimating fractal dimensions in the isotropic case even when the covariance function is anisotropic. Some conditions on $\{u_{ij}\}$ appear necessary for estimator (4.3) to have negligible bias. Under the appropriate conditions on $\{u_{ij}\}$, the Davies and Hall method should perform similarly to the method derived from the joint linear model

$$\log\{\hat{v}_A(u_{ij}\theta_i)\} = \log\{2\,c(\theta_i)\} + \alpha\ \log(u_{ij}) + \text{noise},$$

with a common slope and difference intercepts.

This joint linear model does not use the smoothness information of the function $c(\cdot)$. An alternative idea is to regard this model as a partially linear model and to apply a partially linear estimation technique. The basic idea is first to apply a linear smoother to estimate $c(\cdot)$ by pretending that $\alpha$ is known and then to substitute the estimated function $c(\cdot)$ into the partial linear model to estimate the coefficient $\alpha$. See for example Speckman (1988). Such a method uses the continuity of the function $c(\cdot)$ and is expected to be more efficient.

There are sufficient data for estimating the fractal index $\alpha$ in the partially linear model. Thus, a robust proposal is first to use the method for the anisotropic case and then to examine whether the covariance function is isotropic. The second step amounts to testing a linear model against a partially linear model. In a different context, Fan and Huang (1998) provide a powerful test for this problem based on the adaptive Neyman test.

**D. M. Titterington** (*University of Glasgow*)

It is a pleasure to comment briefly on this interesting paper, which offers an approach of considerable potential for characterizing surface texture at a certain level of detail. The procedures for both point and interval estimation seem both to be of considerable practical utility.

I must admit to being a fractal naïf, and my specific question may betray this, but I have wondered about the possible influence of extraneous noise and pixel-related discretization. To what extent might such factors interfere with the reliability of the methodology?

Of course, the image processing literature is full of methods for characterizing texture, and science abounds with particular problems seeking such analysis. For instance, I am involved with others

in Glasgow (John Chapman in the Department of Physics and Astronomy and Ilya Molchanov and Changjing Shang in the Department of Statistics) in the examination of the progression of a magnetization ripple phenomenon when ferromagnetic multilayers are subjected to a varying applied magnetic field. As the strength of the applied field changes, the resultant effect of the applied field and the properties of the material are revealed as an imaged ripple effect that rotates in the image frame and, more importantly, changes in texture. It is of considerable practical interest to summarize the resulting sequence of images concisely. We are trying various approaches, both involving an empirical application of statistical constructs, such as Markov random fields, and based on the underlying physical theory, although it turns out that an ideal, physics-based attack is not feasible. The nature of our images suggests, in comparison with the examples in the paper, that the ideas of the paper could be relevant to our problem, and we are looking forward to trying them out.

**Trevor F. Cox** (*University of Newcastle*)
Having only recently advanced from knowing fractals as spectacular plots exhibiting striking patterns to an understanding of some of the basic mathematics behind them, this paper attracted my attention. I wish to congratulate the authors on an illuminating account of how fractals can be used for the analysis of surface roughness. As a newcomer to the area I wish to make the following points which may be somewhat naïve, and two of them have already been mentioned by the proposer and seconder of the vote of thanks.

Firstly, I understand that, for some finished surfaces such as those from grinding, honing, lapping and superfinishing, surface heights are negatively skewed. What does this mean for a Gaussian random field assumption and the definition of fractal dimension? Secondly, it could be argued that surface roughness is best measured by second-order properties and that two-dimensional spectral analysis (see for example Renshaw and Ford (1983)) would be more appropriate than a fractal analysis. Lastly, is the self-similar pattern exhibited by fractals, as one delves increasingly deeper into the fractal, realistic in practice? Do surfaces behave differently at different scales of magnification?

The following contributions were received in writing after the meeting.

**Michael J. Phillips** (*University of Leicester*)
It was a great pleasure to be present when this paper by Davies and Hall was read to the Society as it maintains the strong statistical links between Australia and the UK. It is also welcome because of the demonstration of the benefit of the collaboration between statistical science and engineering. In particular I thought that this was powerfully demonstrated by the elegant proof of the *main result* in theorem 1. The authors advocate the use of fractal methodology for the analysis of data from surfaces. As Whitehouse (1994) states these methods are best when representing growth- or death-type mechanical phenomena and hence there must be reservations about the appropriateness of this methodology for surfaces produced by other phenomena.

My own contribution to surface metrology has been limited to the application of parametric modelling of the discrete properties of engineering surfaces (e.g. Whitehouse and Phillips (1982)). However, I wish to invite the authors to comment on the definition of *topothesy*. In Whitehouse (1994) the definition of topothesy $\Lambda$ is connected to the Davies and Hall definition $c$ by

$$c = \tfrac{1}{2}\Lambda^{2D-2}$$

where $D$ is the *fractal dimension*. Then the intercept estimate of $\log(2c)$ in the ordinary least squares linear regression of the structure function is equivalent to an estimate of $(2D-2)\log(\Lambda)$, as suggested by Whitehouse (1994). What are the merits of the different definitions? Does the use of the ordinary least squares linear regression of the structure function make one definition preferable to the other?

**T. R. Thomas** (*Chalmers Tekniska Högskola, Göteborg*)
Our own measurements (Amini *et al.*, 1998) on a strongly anisotropic rough surface (a ground gear tooth) confirm the authors' predictions. We found that in most angular directions the fractal dimension varied between about 1.42 and 1.45, but within a degree or two of the lay it fell to about 1.23. The behaviour of the topothesy (using Berry's definition of the interval at which the mean slope would be 1 rad) was even more dramatic: from a value of $10^{-5}$–$10^{-6}$ mm in most angular directions, it fell sharply in the direction of the lay to about $10^{-11}$ mm. It would be helpful to tribologists and others if the authors could produce quantitative estimates of the behaviour of the topothesy for comparison.

However, Doege *et al.* (1996), using a Hurst orientation transform (see for example Russ (1994)) to measure the fractal dimension of a strongly anisotropic sheet metal surface, found a smooth progressive change, from $D \cong 1.46$ across the lay to $D \cong 1.34$ parallel to the lay. This seems in contradiction both to the present authors' predictions and to our own measurements. We would be interested to hear their comments on Doege's work.

**Keming Yu** (*Lancaster University*)

Much of spatial analysis lies in predicting the underlying spatial surface $S(\mathbf{x})$, say, at the location $\mathbf{x}$, which is usually assumed a stationary Gaussian process with $E[S(\mathbf{x})] = \mathbf{0}$ and

$$\text{cov}\{S(\mathbf{x}), S(\mathbf{x}')\} = \sigma^2 \rho(\mathbf{x} - \mathbf{x}').$$

Here $\rho(t) \equiv \rho_{\theta_1,\theta_2}(t)$ is usually specified by a pair of parameters $(\theta_1, \theta_2)$. One of the parameters characterizes the roughness of the surface, and the other controls the spatial range of correlation. For example, $\rho(t) = \exp(-\alpha|t|^{\delta})$ with $(\theta_1, \theta_2) = (\alpha, \delta)$. Further, $\rho(t)$ usually satisfies

$$\rho(t) = \rho(0) - \theta_1 \|t\|^{\theta_2} + O(\|t\|^{\theta_2}),$$

so $\theta_2$ can be regarded as a fractal index and $\theta_1$ is the topothesy. There are many methods for estimating these parameters; see, for example, Cressie (1991) and Ripley (1981). In particular, a Bayesian approach provides a way of incorporating parameter uncertainty (see Handcock and Stein (1993) and Diggle *et al.* (1998)). I just wonder whether these methods can be employed to estimate the fractal dimension in some practical cases. However, some intensive parameter estimating methods such as applying Markov chain Monte Carlo methods for fitting a parametric model for the covariance structure of a spatial surface are quite time consuming in practice. Can fractal methods be used for parameter estimation of the covariance structure in some spatial analyses? How different is the fractal method from those ready made estimating methods in terms of estimating precision and incorporating parameter uncertainty?

The **authors** replied later, in writing, as follows.

We are grateful for Taylor's interesting and helpful comments. We agree that software for fitting piecewise linear curves to data, and recording the total length of each fit, would be useful. On the matter of fits to log–log-plots at increasingly finer resolution levels, we note that for many types of data the manner of recording provides a definite bound to the utility of such fits. For example, in the case of data recorded by stylus or optical profilometry, the diameter of the stylus or light beam can severely restrict the type of information that may be extracted from high resolution data. Note also that the way in which surface profile information is 'convolved' (for want of a better word) with the shape of a stylus is quite non-linear, making 'deconvolution' particularly difficult. This also responds to one of Cox's points, about the results of exploring rough surfaces at very high levels of resolution.

Taylor and Ripley, and perhaps also Cox, query our assumption following equation (2.2) that the process $X$ be 'sufficiently closely related to a Gaussian field (see Hall and Roy (1994) for discussion and regularity conditions)'. Of course, that assumption does not require $X$ to be itself Gaussian. As Hall and Roy (1994) showed, a great many smooth functions of jointly distributed, fractal Gaussian fields are covered by this statement, including $\chi^2$-processes and many others besides. Therefore, for example, Ripley's concern that 'samples from Gaussian series look the same when reversed and with a sign change' seems unnecessary. Indeed, the very asymmetry of $\chi^2$-processes makes them ideal for modelling worn surfaces in some settings; see for example Hall and Roy (1994). This also responds to a comment made by Cox.

The correlation of residuals, noted by Taylor, is an issue in testing hypotheses or constructing confidence regions, but it is implicitly taken into account by our bootstrap approach to these procedures, provided that the model from which one simulates is appropriate. The model may itself be tested by Monte Carlo means. Heavy-tailed departures from Gaussianity are discussed in the context of fractal analysis of exchange rate data by Hall *et al.* (1996). The example there is of particular interest since the observed data appear to have been generated by a fractal process with sample paths of the same dimension as a Wiener process, but the marginal distribution has significantly heavier tails than the Wiener assumption would allow. Classical theory describing exchange rate fluctuations is built around the Wiener model.

We agree with Taylor that generalized and weighted least squares are viable alternatives to the methods that we used. We did not employ them in our paper for reasons that are discussed towards the

end of Section 1.1. See also our response to Wood and Chan below.

There is no difficulty in developing bootstrap tests for stationarity and isotropy, as suggested by Taylor. They are in fact contained in Davies (1998), and their conclusions justify the claims made in the paper under discussion — in particular, the decision to treat the soil surface data as isotropic. Also, we have tested for differences of fractal dimension in directions of greatest roughness and did not obtain statistically significant results.

Unfortunately it is seldom practical to align the direction in which the roughness is greatest with an axis of the pixel lattice, as Taylor suggests. For one thing, the information that is needed to determine the appropriate direction is often not available until the data have been recorded and analysed — so the issue of the order of carts and horses must be considered. Moreover, it can be virtually impossible to align samples in the desired way. This is the case for the plastic sheet data, for example, whose recording required intricate physical manipulations of small pieces of material at close to the molecular level.

We appreciate Ripley's thought-provoking remarks. Like him we do not 'believe' in fractals, if believing means an acceptance that natural phenomena actually have fractal properties. However, like G. E. P. Box we believe that although all theoretical models are invalid, many are useful. Fractal properties of physical surfaces evidence themselves in many ways (see for example Figs 7 and 11). By exploiting those features we may obtain valuable information about both the surfaces themselves and the processes that produced them.

In reply to Ripley's final point, about whether the $u_i$ depend on $n$, the answer is that they do. See for example Sections 5.2 and 5.3, and in particular condition (5.6). The regularity conditions in Section 5 also provide a response to a remark by Fan and Yao, concerning the $u_{ij}$.

The comments of Wood and Chan are particularly interesting to us. The generalized or weighted approach to analysis is particularly attractive from a theoretical viewpoint, but numerically it does not enjoy the promise that the theory suggests. And in the case of two dimensions there are even greater complexities in choosing the weights than exist in one dimension. It is not clear to us quite why practice does not live up to expectation from the theory, except that it seems to have something to do with the high degree of correlation of many of the quantities involved (e.g. correlations of variogram estimates at neighbouring lags). This results in relatively high order terms having much greater influence than they 'should', until the sample size is large.

On the matter of statistical performance, it should be mentioned that in many contexts where fractal data are recorded by machine the expense of increasing the sample size by even several fold can be minimal, provided that the decision is made before recording actually starts. (Setting up a second time, to record more data from the same source, can be relatively expensive.) Therefore, the traditional statistical trade-off of actual statistical benefit *versus* theoretically optimal performance tends, in problems involving fractal analyses, to come down more in favour of relatively simple conservative methods that are known to perform well than it might in other contexts.

In response to Titterington's very pertinent comments, we should mention that discretization error is usually evident from the fact that the graph of the logarithm of the variogram against the logarithm of the lag is concave for small values of the lag. Noise, in contrast, tends to be characterized by convexity for small lags. Neither of these trends is evident in our data. If they had been, we would not have fitted our straight lines as close to the origin as we do in Figs 7 and 11.

After inspecting Titterington's ferromagnetic data, it seems to us very likely that the electromagnetic fields that are responsible for generating the patterns to which he refers can be classified in terms of their fractal properties.

In response to Phillips's remark about the definition of topothesy $\Lambda$, we note that Whitehouse and Phillips (1982) defined it to be the solution of $v(\Lambda) = \Lambda^2$, where $v$ denotes the variogram. (Actually, they employed an estimator of $v$.) Therefore, if $c$ represents our definition of topothesy, then the formula $c = \frac{1}{2}\Lambda^{2D-2}$, given by Phillips, is valid if the process $X$ is self-similar, but not otherwise. Our definition of topothesy in terms of the behaviour of $v$ at the origin, or equivalently in terms of fluctuations of $X$ on an infinitesimally fine scale, enables ready comparisons to be made of roughness levels for different processes (self-similar or otherwise) with fractal properties. There are, however, advantages in defining topothesy as $c' = c^{1/\alpha}$, or equivalently $c' = c^{1/2(2-D)}$ if $d = 1$, since then, multiplying the units of $t$ by a constant amounts to dividing the units of $c'$ by the same amount.

We are particularly gratified by Thomas's remark that our theoretical assertions about the variation in fractal dimension with orientation are in good agreement with his own observations for ground metal surfaces. Cases where the theory is in dispute with data sometimes arise because the observed surface cannot be adequately modelled by a *stationary* process.

The present paper does not address in any detail the statistical properties of dimension and topothesy for 'ruled' surface problems, such as those mentioned by Thomas. Departures from the mathematical ideal of a ruled surface need to be modelled and studied in their own right, and we plan to investigate them in the near future.

The alternative approaches suggested by Fan and Yao deserve further analysis. Bootstrap and Monte Carlo methods can be employed to test for anisotropy, and Fan and Yao's ideas can be developed in this context. Yu is of course right in suggesting that other techniques may also be employed. We point out, however, that the most appropriate fractal 'model' for a covariance is usually only semiparametric, in the sense that remainder terms of smaller order than $\|t\|^{\alpha}$ would usually not be specified.

## References in the discussion


Amini, N., Rosén, B.-G. and Thomas, T. R. (1998) Fractal surfaces characterised by a 3D structure function. In *Proc. Fractal '98*. To be published.

Appleyard, S. T., Witkowski, J. A., Ripley, B. D., Shotton, D. M. and Dubowicz, D. (1985) A novel procedure for pattern analysis of features present on freeze fractured plasma membranes. *J. Cell Sci.*, **74**, 105–117.

Chan, G. and Wood, A. T. A. (1997) Increment-based estimators of fractal dimension for two-dimensional surface data. *Statist. Sin.*, to be published.

Constantine, A. G. and Hall, P. (1994) Characterizing surface smoothness via estimation of effective fractal dimension. *J. R. Statist. Soc.* B, **56**, 97–113.

Cressie, N. (1985) Fitting variogram models by weighted least squares. *J. Int. Ass. Math. Geol.*, **17**, 563–586.

——— (1991) *Statistics for Spatial Data*. New York: Wiley.

Davies, S. (1998) The stochastic analysis of surface roughness — a fractal-based approach. *PhD Thesis*. Australian National University, Canberra.

Davis, B. M. and Borgman, L. E. (1979) Some exact sampling distributions for variogram estimators. *J. Int. Ass. Math. Geol.*, **14**, 189–193.

Diggle, P. J., Tawn, J. A. and Moyeed, R. A. (1998) Model-based geostatistics (with discussion). *Appl. Statist.*, **47**, 299–350.

Doege, E., Othmani, A. and Kaminski, C. (1996) Fractal investigations of sheet metal surfaces. In *Proc. 4th Eur. Conf. Intelligent Techniques and Soft Computing*, pp. 1737–1742. Aachen: Elite Foundation.

Fan, J. and Huang, L. (1998) Goodness-of-fit test for parametric regression models. In *Institute of Statistics Mimeo Series*. Chapel Hill: University of North Carolina.

Ford, E. D. (1976) The canopy of a Scots pine forest: description of a surface of complex roughness. *Agric. Meteorol.*, **17**, 9–32.

Hall, P., Matthews, D. and Platen, E. (1996) Algorithms for analyzing nonstationary time series with fractal noise. *J. Comput. Graph. Statist.*, **5**, 351–364.

Hall, P. and Roy, R. (1994) On the relationship between fractal dimension and fractal index for stationary stochastic processes. *Ann. Appl. Probab.*, **4**, 241–253.

Handcock, M. S. and Stein, M. L. (1993) A Bayesian analysis of kriging. *Technometrics*, **35**, 403–410.

Kent, J. T. and Wood, A. T. A. (1997) Estimating the fractal dimension of a locally self-similar Gaussian process by using increments. *J. R. Statist. Soc.* B, **59**, 679–699.

Mandelbrot, B. B. (1977) *Fractals: Form, Chance and Dimension*. San Francisco: Freeman.

——— (1982) *The Fractal Geometry of Nature*. San Francisco: Freeman.

Renshaw, E. and Ford, E. D. (1983) The interpretation of process from pattern using two-dimensional spectral analysis: methods and problems of interpretation. *Appl. Statist.*, **32**, 51–63.

Richardson, L. F. (1961) The problem of contiguity: an appendix of statistics of deadly quarrels. *Gen. Syst. Yearbk*, **6**, 139–187.

Ripley, B. D. (1981) *Spatial Statistics*. New York: Wiley.

——— (1985) Discussion on Spatial structure and spatial interaction: modelling approaches to the statistical analysis of geographical data (by R. J. Bennett and R. P. Haining). *J. R. Statist. Soc.* A, **148**, 27–28.

——— (1988) *Statistical Inference for Spatial Processes*. Cambridge: Cambridge University Press.

Russ, J. C. (1994) *Fractal Surfaces*. New York: Plenum.

Speckman, P. (1988) Kernel smoothing in partial linear models. *J. R. Statist. Soc.* B, **50**, 413–436.

Taylor, C. C. and Taylor, S. J. (1991) Estimating the dimension of a fractal. *J. R. Statist. Soc.* B, **53**, 353–364.

Whitehouse, D. J. (1994) *Handbook of Surface Metrology*. Bristol: Institute of Physics.

Whitehouse, D. and Phillips, M. J. (1982) Two-dimensional discrete properties of random surfaces. *Phil. Trans. R. Soc. Lond.* A, **305**, 441–468.